Comput. Methods Appl. Mech. Engrg. 198 (2009) 3975–3988

Contents lists available at ScienceDirect

Comput. Methods Appl. Mech. Engrg.

journal homepage: www.elsevier.com/locate/cma

Grad–div stabilization and subgrid pressure models for the incompressible Navier–Stokes equations

Maxim Olshanskii [a,*,1], Gert Lube [b], Timo Heister [b,2], Johannes Löwe [b,2]

[a] Department of Mechanics and Mathematics, Moscow State M.V. Lomonosov University, Russia
[b] Department of Mathematics and Computer Science, Georg-August University, Göttingen, D-37083, Germany

ARTICLE INFO

Article history:
Received 24 June 2009
Received in revised form 31 August 2009
Accepted 3 September 2009
Available online 11 September 2009

Keywords:
Navier–Stokes
Finite elements
Variational multiscale method
Stabilized method
Stabilization parameters

ABSTRACT

In this paper the grad–div stabilization for the incompressible Navier–Stokes finite element approximations is considered from two different viewpoints: (i) as a variational multiscale approach for the pressure subgrid modeling and (ii) as a stabilization procedure of least-square type. Some new error estimates for the linearized problem with the grad–div stabilization are proved with the help of norms induced by the pressure Schur complement operator. We discuss the stabilization parameter choice arising in the frameworks of least-square and multiscale methods and consider assumptions which allow to relate both approaches.

1. Introduction

Numerical simulation of laminar and turbulent incompressible flows is an important subtask in many industrial applications and remains within the focus of intensive scholar research. Incompressible viscous flows of a Newtonian fluid are modeled by the system of the Navier–Stokes equations, which read: Given a bounded, connected domain $\Omega \subset \mathbb{R}^d$ $(d = 2,3)$ with a piecewise smooth boundary $\partial\Omega$, the simulation time T, and a force field $\mathbf{f} : (0,T] \times \Omega \to \mathbb{R}^d$, find a velocity field $\mathbf{u} : (0,T] \times \Omega \to \mathbb{R}^d$ and a pressure field $p : (0,T] \times \Omega \to \mathbb{R}$ such that

$$\frac{\partial \mathbf{u}}{\partial t} - \nu\Delta\mathbf{u} + (\mathbf{u}\cdot\nabla)\mathbf{u} + \nabla p = \mathbf{f} \quad \text{in } (0,T] \times \Omega, \tag{1}$$

$$\operatorname{div}\mathbf{u} = 0 \quad \text{in } [0,T] \times \Omega, \tag{2}$$

$$\mathbf{u}|_{t=0} = \mathbf{u}_0 \quad \text{in } \Omega, \tag{3}$$

where $\nu > 0$ is the kinematic viscosity coefficient. Some boundary conditions have to be imposed on $\partial\Omega$ to obtain a closed set of equations.

Among various discretization techniques for the Navier–Stokes equations the finite element (FE) method is one of the most popular and mathematically sound variants. Nevertheless, it is well-known that FE methods for (1)–(3) may suffer from several sources of instabilities. One is a possible incompatibility of pressure and velocity FE pairs. A remedy is a choice of FE spaces passing the inf–sup or LBB condition [8] or the use of pressure stabilizing techniques [25]. Another source of instabilities stems from domination of advection terms over viscous terms, which is typically characterized by large mesh Reynolds numbers. This shortcoming can be overcome to some extent by a variety of stabilizing techniques, including streamline-upwind Petrov–Galerkin, the use of residual-free bubbles enrichment, local projection stabilization, and interior-penalty methods, see, e.g. [6,10–12]. There exist several variants of stabilized FE methods of arbitrary accuracy order which simultaneously suppress instabilities caused by both, dominating advection and non-LBB-stable FE spaces, see, e.g. [14,18,24,26]. Besides being widely used these methods enjoy nowadays a solid mathematical foundation, e.g. [44].

While the instability caused by dominating advection terms can be related to the failure of a given mesh to resolve sharp layers (small scales) in velocity, there is another less well-studied instability source in the Galerkin discretization method related to a possible poor resolution of pressure. Due to connections between variables already present in the linear Stokes problem, the loss of accuracy in pressure may destructively affect the velocity approximation in a way that *Velocity Error* $\sim$ *Re* $*$ *Pressure Error*, cf. [41] and Remark 8. In laminar flows, the kinematic pressure is often a

* Corresponding author. Tel.: +7 495 9393834.
E-mail addresses: Maxim.Olshanskii@mtu-net.ru (M. Olshanskii), lube@math.uni-goettingen.de (G. Lube).

[1] Partially supported by the Russian Foundation for Basic Research through the projects 08-01-00415, 09-01-00115 and RAS Program “Contemporary Problems of Theoretical Mathematics” through the Project No. 01.2.00104588.

[2] Partially supported by the German Research Foundation (DFG) through Research Training Group GK 1023.

0045-7825/$ - see front matter © 2009 Elsevier B.V. All rights reserved.
doi:10.1016/j.cma.2009.09.005

(much) more smooth function than the velocity; hence this instability phenomenon is less pronounced, especially if equal-order discretizations are applied to model flows with moderate Reynolds numbers. This can be a reason why the phenomenon has not drawn much attention in the FE literature until recently. If inf–sup stable elements are used, then the LBB condition places a strong link between velocity and pressure degrees of freedom. This condition roughly implies that, for higher order elements, the polynomial degree of pressure approximations is less than the polynomial degree of velocity approximations. In this case the pressure may be under-resolved by lower order polynomials and an additional modeling for suppressing the related instability is needed [7,20,29,40]. The situation becomes even more critical if the formulation of the Navier–Stokes equations involves the Bernoulli pressure variable[3]. The Bernoulli pressures exhibit the same complex dynamic as velocities and if a mesh fails to resolve it, an additional stabilization is vital [30,31,40]. Such instabilities can be suppressed with the grad–div stabilization introduced below.

Assume a finite element partition $\{\mathcal{T}_h\}$ of Ω and conforming FE spaces for velocities and pressures $\mathbf{V}_h$ and $\mathbb{Q}_h$. Consider the semi-discrete version of (1)–(3): Find $\{\mathbf{u}_h, p_h\} \in \mathbf{V}_h \times \mathbb{Q}_h\ \forall t \in (0, T]$ solving

$$\begin{aligned}&\left(\frac{\partial \mathbf{u}_h}{\partial t}, \mathbf{v}_h\right) + \nu(\nabla \mathbf{u}_h, \nabla \mathbf{v}_h) + ((\mathbf{u}_h \cdot \nabla)\mathbf{u}_h, \mathbf{v}_h) - (p_h, \operatorname{div} \mathbf{v}_h)\\ &\quad + (q_h, \operatorname{div} \mathbf{u}_h) + \sum_{K \in \mathcal{T}_h} \gamma_K \int_K \operatorname{div} \mathbf{u}_h \operatorname{div} \mathbf{v}_h \, d\mathbf{x}\\ &\quad = (\mathbf{f}, \mathbf{v}_h) \quad \forall \{\mathbf{v}_h, q_h\} \in \mathbf{V}_h \times \mathbb{Q}_h, \quad \forall t \in (0, T]. \end{aligned} \tag{4}$$

We use the notation $(\cdot,\cdot)$ for the scalar product in $L^2(\Omega)^k,\ k = 1, 2, \ldots$. The choice of element dependent parameters $\gamma_K \geqslant 0$ defines the last term on the left-hand side of (4); $\gamma_K = 0$ for all elements K corresponds to the plain Galerkin method. Adding such a term is known as *the grad–div stabilization* (the name reflects the fact that adding $-\nabla\gamma \operatorname{div} \mathbf{u}$ with varying γ to (1) can be seen as the continuous counterpart of the stabilization). Parameters γ_K are constant on each element and each time $t \in (0, T]$, but may in general depend on t and the discrete solution $\mathbf{u}_h, p_h$, leading in the latter case to a non-linear stabilization.

Remark 1. To focus the discussion and analysis below we intentionally do not include any other stabilization terms in (4) and further on. However this still may be needed in practice in order to stabilize the advection operator and/or allow arbitrary velocity–pressure FE pairs. In fact, including such terms does not alter the main results and conclusions of this paper.

Generally speaking, adding the penalization of the continuity constraint to the FE formulation is not a new idea at all. These terms are part of the streamline-upwinding Petrov–Galerkin method (SUPG) in [18,24]. However, in practice these terms are often omitted, and until recently it was not clear if they are needed for technical reasons of the analysis of SUPG type methods only or play an important role in computations. The role of the grad–div stabilization was again emphasized in recent studies of (stabilized) FE methods for incompressible flow problems, see [7,29,37,38,40,41,46], also in conjunction with the rotation form in [30,31,40]. Its relation to the variational multiscale approach was revealed in [14,22]. In particular, numerical studies in [29] and [31] show that the grad–div stabilization is highly important for the practical use of some turbulence models (both with convection and rotation forms of non-linearities).

[3] A different from (1) formulation is based on the identity $(\mathbf{u} \cdot \nabla)\mathbf{u} = \operatorname{rot} \mathbf{u} \times \mathbf{u} + \nabla \frac{\mathbf{u}^2}{2}$ and $P = \frac{\mathbf{u}^2}{2} + p$ as the new pressure variable (Bernoulli pressure) leading to what is known as the rotation form of the N.-S. eqs. This form is widely used in turbulence modeling. For example, a popular and well-mathematically supported NS-alpha model [17] of turbulence uses the rotation form.

At the same time, the right choice of parameters γ_K remains a controversial issue. Few receipts can be found in the literature, but the question of there relevance and optimality remains open.

In this paper, the grad–div stabilization for the incompressible Navier–Stokes finite element approximations is considered from two different viewpoints:

(i) as a variational multiscale approach for the pressure subgrid modeling and
(ii) as a stabilization procedure of least-square type.

We discuss the design of parameters γ_K arising in the frameworks of least-square and multiscale methods and look for assumptions which allow to relate both approaches. In particular, we show that currently adopted assumptions in the multiscale framework lead to some inconsistency in the choice of γ's. Using the least-square framework we prove an error estimate for the grad–div stabilized finite element method applied to the linearized Navier–Stokes problem. Moreover, with the help of norms induced by the pressure Schur complement operator we show that, in the Stokes case, the estimate is optimal in a certain sense. The estimate leads to an 'optimal' choice of γ_K, which is based, however, on higher-order norms of the unknown continuous solution. To obtain computationally feasible formulas we introduce different modeling assumptions. Doing this we are able to show the interrelation of different receipts known from the literature, to identify the possible limitations of their applicability and to deduce few improved formulas.

As a prototypical model for our studies we adopt the steady linearized Navier–Stokes problem (the Oseen problem) with homogeneous Dirichlet boundary conditions given by:

$$\begin{aligned} &-\nu\Delta\mathbf{u} + \mathbf{a} \cdot \nabla \mathbf{u} + \nabla p = \mathbf{f} \quad \text{in } \Omega,\\ &\operatorname{div} \mathbf{u} = 0 \quad \text{in } \Omega,\\ &\mathbf{u} = 0 \quad \text{on } \partial\Omega. \end{aligned} \tag{5}$$

The mean value condition $\int_\Omega p \, d\mathbf{x} = 0$ should be imposed to make the pressure solution unique; $\mathbf{a}$ is a given approximation of the solution from the previous time step or non-linear iteration. For the sake of analysis we assume $\mathbf{a} \in L^\infty(\Omega)^d$, $\operatorname{div} \mathbf{a} = 0$.

The remainder of the paper is organized as follows: In Section 2, we discuss the grad–div stabilization as a subgrid pressure model in the framework of variational multiscale methods. Then, Section 3 provides refined error estimates of the grad–div stabilized method for linearized problems of Stokes and Oseen type. The problem of numerical dissipation and mass balance for grad–div terms is discussed in Section 4. Finally, some numerical experiments for the Oseen and the Navier–Stokes problem are given in Section 5.

2. Grad–div stabilization and the subgrid modeling

In this section, the grad–div stabilization is observed as a subgrid pressure model in the framework of the variational multiscale method of Hughes and coauthors [2,27,28]. We will show that current models known from the literature lead, however, to a somewhat questionable conclusion for the unresolved subgrid pressure behavior and hence to a possibly inconsistent design of γ's. Define the following spaces

$$\mathbf{V} := \{\mathbf{v} \in H^1(\Omega)^d | \mathbf{v} = 0 \text{ on } \partial\Omega\}, \quad \mathbb{Q} := \left\{q \in L^2(\Omega) | \int_\Omega q \, d\mathbf{x} = 0\right\}$$

and the bilinear form

$$a(\mathbf{u}, p; \mathbf{v}, q) = \nu(\nabla \mathbf{u}, \nabla \mathbf{v}) + (\mathbf{a} \cdot \nabla \mathbf{u}, \mathbf{v}) - (p, \operatorname{div} \mathbf{v}) + (q, \operatorname{div} \mathbf{u}).$$

The weak formulation of the Oseen problem (5) reads: Given $\mathbf{f} \in L^2(\Omega)^d$ find $\mathbf{u} \in \mathbf{V}$ and $p \in \mathbb{Q}$ such that

$$a(\mathbf{u}, p; \mathbf{v}, q) = (\mathbf{f}, \mathbf{v}) \quad \forall\, \mathbf{v} \in \mathbf{V},\ \ q \in \mathbb{Q}. \tag{6}$$

For the discretization of (5) we introduce a family $\mathscr{T}_h$ of triangulations of Ω (triangles or quadrilaterals in 2D, tetrahedra or hexahedral elements in 3D) without hanging nodes, parameterized with mesh size parameter $h = \max_{K\in\mathscr{T}} h_K$, and $h_K = \mathrm{diam}(K)$. We use conforming finite elements with piecewise polynomial functions. This results in FE spaces $\mathbf{V}_h$ and $\mathbb{Q}_h$ for velocity and pressure.

Consider the orthogonal decomposition of pressure and velocity spaces (e.g., H^1-orthogonal for $\mathbf{u}$ and L^2-orthogonal for p):

$$\mathbf{V} = \mathbf{V}_h \oplus \widetilde{\mathbf{V}}, \quad \mathbb{Q} = \mathbb{Q}_h \oplus \widetilde{\mathbb{Q}}.$$

Let $\{\mathbf{u}, p\}$ be the strong solution of the Oseen equations (5). We have the decomposition of the solution on resolved and unresolved parts:

$$\mathbf{u} = \mathbf{u}^h + \tilde{\mathbf{u}}, \quad p = p^h + \tilde{p}. \tag{7}$$

In general, $\mathbf{u}^h, p^h$ in (7) are unknown and we are looking for equations which allow us to find an accurate approximation to $\mathbf{u}^h, p^h$. Testing the weak formulation of the Oseen problem (6) with arbitrary $\{\mathbf{v}_h, q_h\} \in \mathbf{V}_h \times \mathbb{Q}_h$ we get

$$a(\mathbf{u}^h, p^h; \mathbf{v}_h, q_h) + a(\tilde{\mathbf{u}}, \tilde{p}; \mathbf{v}_h, q_h) = (\mathbf{f}, \mathbf{v}_h) \quad \forall\, \mathbf{v}_h \in \mathbf{V}_h,\ q_h \in \mathbb{Q}_h. \tag{8}$$

With $\langle \cdot; \cdot \rangle$ standing for a L^2-duality pairing between $\mathbf{V} \times \mathbb{Q}$ and $\mathbf{V}^* \times \mathbb{Q}$, and $\mathscr{L}^*$ for the adjoint of the Oseen operator

$$\mathscr{L} := \begin{bmatrix} -\nu\Delta + \mathbf{a}\cdot\nabla & \nabla \\ -\mathrm{div} & 0 \end{bmatrix}, \tag{9}$$

Eq. (8) can be rewritten as

$$a(\mathbf{u}^h, p^h; \mathbf{v}_h, q_h) + \langle \tilde{\mathbf{u}}, \tilde{p}; \mathscr{L}^*[\mathbf{v}_h, q_h]^t \rangle = (\mathbf{f}, \mathbf{v}_h) \quad \forall\, \mathbf{v}_h \in \mathbf{V}_h,\ \ q_h \in \mathbb{Q}_h. \tag{10}$$

Furthermore, since $\mathbf{u}^h, p^h$ are polynomials in any $K \in \mathscr{T}_h$ and $\{\mathbf{u}, p\}$ is the strong solution, it holds

$$\mathscr{L}\begin{bmatrix} \tilde{\mathbf{u}} \\ \tilde{p} \end{bmatrix} = \begin{bmatrix} \mathbf{f} \\ 0 \end{bmatrix} - \mathscr{L}\begin{bmatrix} \mathbf{u}^h \\ p^h \end{bmatrix} \quad \text{in } K \tag{11}$$

for all $K \in \mathscr{T}_h$. To ensure the well-posedness of (11) on each element K as a problem for unresolved scales one has to supply some additional conditions, for example

$$\tilde{\mathbf{u}}|_{\partial K} = (\mathbf{u} - \mathbf{u}^h)|_{\partial K} \quad \text{and} \quad \int_K \tilde{p}\, d\mathbf{x} = \int_K (p - p^h)\, d\mathbf{x}. \tag{12}$$

Up to this point (5) is clearly equivalent to the set of Eqs. (10)–(12). Now the intention is to obtain from (10) an equation only for the resolved scales $\mathbf{u}^h, p^h$ in a way that the influence of the unresolved scales through the second term in (10) is modeled. To this end, one typically accepts several simplifications in order to deduce from (11) simple expressions for $\tilde{\mathbf{u}}$ and $\tilde{p}$ in terms of resolved scales residual $[\mathbf{f}, 0]^t - \mathscr{L}[\mathbf{u}^h, p^h]^t$. Below we outline some typical modelling assumptions:

Assumption 1. Following [9,22,27,28,35,39] one may assume that the unresolved velocity vanishes on element boundaries:

$$\tilde{\mathbf{u}}|_{\partial K} = 0. \tag{13}$$

It is also natural to assume the zero mean of the unresolved pressure on every K:

$$\int_K \tilde{p}\, d\mathbf{x} = 0. \tag{14}$$

Assumption (13) is rather strong, although in [43] it is argued that, for small enough h_K, this should not introduce a significant modeling error. In some variational multiscale models a similar assumption is made less explicit by neglecting boundary integrals arising in integration by parts relations, as for example in the second term in (10).

Note that (11) with (13),(14) is a well-posed problem for $\tilde{\mathbf{u}}$ and $\tilde{p}$.

Another common simplification is assuming that, for all elements $K \in \mathscr{T}_h$, the Oseen operator $\mathscr{L}$ from (9), which has a natural 2×2 block structure, can be reasonably well-approximated by a block-diagonal one, see e.g. [2,14,22]. This is the same as admitting:

Assumption 2. $\tilde{\mathbf{u}}$ depends only on the residual of momentum equation in $[\mathbf{f}, 0]^t - \mathscr{L}[\mathbf{u}^h, p^h]^t$ and $\tilde{p}$ depends only on the residual of the continuity equation:

$$\begin{bmatrix} \tilde{\mathbf{u}} \\ \tilde{p} \end{bmatrix} \approx \begin{bmatrix} \mathscr{L}_u & 0 \\ 0 & \mathscr{L}_p \end{bmatrix} \left(\begin{bmatrix} \mathbf{f} \\ 0 \end{bmatrix} - \mathscr{L}\begin{bmatrix} \mathbf{u}^h \\ p^h \end{bmatrix} \right) \quad \text{for all } K \in \mathscr{T}_h. \tag{15}$$

The simplification coming from (15) is not completely *ad hoc*: for example, from the theory of algebraic saddle point problems it is well-known that, multiplying $\mathscr{L}$ with such block-diagonal approximations, leads to a matrix with well-clustered eigenvalues if $\mathscr{L}_u^{-1}$ and $\mathscr{L}_p^{-1}$ are good approximations to velocity (1,1)-block of $\mathscr{L}$ and the pressure Schur complement operator, respectively, cf. [45]. Thus it is reasonable to set

$$\mathscr{L}_u := (-\nu\Delta + \mathbf{a}\cdot\nabla)^{-1} \quad \text{and}$$
$$\mathscr{L}_p := -(\mathrm{div}\,(-\nu\Delta + \mathbf{a}\cdot\nabla)^{-1}\nabla)^{-1}, \tag{16}$$

where $(-\nu\Delta + \mathbf{a}\cdot\nabla)^{-1}$ is the solution operator for the velocity convection–diffusion problem in element K with boundary conditions from (13).

The final modeling step consists of replacing the operators $\mathscr{L}_u$ and $\mathscr{L}_p$ in (15) on each element K by the scaled identity operators $\tau_K I$ and $\gamma_K I$ where τ_K and γ_K are element-dependent constants [9,27,28]. This leads to:

Assumption 3. Relations (15) are replaced by the model:

$$\tilde{\mathbf{u}} \approx \tau_K(\mathbf{f} + \nu\Delta\mathbf{u}^h - \mathbf{a}\cdot\nabla\mathbf{u}^h - \nabla p^h), \quad \tilde{p} \approx \gamma_K\, \mathrm{div}\,\mathbf{u}^h \quad \text{for all } K \in \mathscr{T}_h. \tag{17}$$

Thanks to (13), (17) and the orthogonality $(\nabla\tilde{\mathbf{u}}, \nabla\mathbf{u}^h) = 0$ we get from (10) the following *discrete model*: Find $\{\mathbf{u}_h, p_h\} \in \mathbf{V}_h \times \mathbb{Q}_h$ solving

$$\begin{aligned} & a(\mathbf{u}_h, p_h; \mathbf{v}_h, q_h) + \sum_{K\in\mathscr{T}_h} \gamma_K \int_K \mathrm{div}\,\mathbf{u}_h\, \mathrm{div}\,\mathbf{v}_h\, d\mathbf{x} + \sum_{K\in\mathscr{T}_h} \tau_K \\ & \quad \times \int_K (-\nu\Delta\mathbf{u}_h + \mathbf{a}\cdot\nabla\mathbf{u}_h + \nabla p_h - \mathbf{f}) \cdot (\mathbf{a}\cdot\nabla\mathbf{v}_h + \nabla q_h)\, d\mathbf{x} \\ & \quad = (\mathbf{f}, \mathbf{v}_h) \quad \forall\, \mathbf{v}_h \in \mathbf{u}_h,\ \ q_h \in \mathbb{Q}_h. \end{aligned} \tag{18}$$

The solution to (18) can be observed as an approximation to $\{\mathbf{u}^h, p^h\}$ from (7) up to the modeling Assumptions 1–3. The third term in (18) models the effect of the unresolved velocity on the resolved velocity and pressure. Its stabilizing effect is well-known for a long time and has been studied within the theory of SUPG-methods [11,18,26]. *The second term in (18) corresponds to the modeling of the effect of unresolved pressure* and coincides with the grad–div stabilization.

One possible way to define the parameters τ_K and γ_K on element K is based on ensuring

$$\tau_K \approx \|\mathscr{L}_u\| \quad \text{and} \quad \gamma_K \approx \|\mathscr{L}_p\|,$$

with $\mathscr{L}_u$ and $\mathscr{L}_p$ from (16). The operator norms are understood as the norms on $L^2(K)$, see [14]. Letting $\mathbf{a}$ be a constant vector on an element K, the Fourier analysis leads to the choice (cf. Remark 1 in [14]): $\tau_K = (c_1 \nu h_K^{-2} + c_2\|\mathbf{a}\|_K h_K^{-1})^{-1}$ and

$$\gamma_K = c_3\nu + c_4\|\mathbf{a}\|_K h_K. \tag{19}$$

with some constants $c_1, \ldots, c_4$.

Note that the order of velocity and pressure finite elements was never taken into account in the considerations above. In particular, the design of γ_K from (19) is assumed for both, equal-order pairs and LBB stable elements of any order. This leads, however, to the following *inconsistency*: From the condition $\operatorname{div}\mathbf{u} = 0$ and (17) we get

$$\tilde{p} \approx -\gamma_K \operatorname{div}\tilde{\mathbf{u}} \quad \text{in } K, \quad \forall K \in \mathscr{T}_h. \tag{20}$$

If γ_K is independent of a relation between the velocity and pressure elements, than $\|\tilde{p}\|$ is completely determined by the resolution properties of the resolved-scale velocity space $\mathbf{V}_h$. This contradicts to the possibility of using both, equal order and different order (LBB stable) elements, for $\mathbf{V}_h \times \mathbb{Q}_h$ with the same sets of parameters. As an example, consider the equal order $P_k - P_k$ and the Taylor–Hood $P_k - P_{k-1}$ pairs for some $k \geqslant 2$ and the same fixed quasi-uniform triangulation $\mathscr{T}_h$, i.e. $h_K \approx h$ for all $K \in \mathscr{T}_h$. Let also $\|\mathbf{a}\|_K = O(1)$ for all $K \in \mathscr{T}_h$, yielding $\gamma_K \approx \gamma$ for all $K \in \mathscr{T}_h$ for some constant $\gamma > 0$. Thanks to (20)

$$\|\tilde{p}\| \approx \gamma\|\operatorname{div}\tilde{\mathbf{u}}\|. \tag{21}$$

The subgrid velocity $\tilde{\mathbf{u}}$ (the projection of $\mathbf{u}$ on $\widetilde{\mathbf{V}}$) is the same function for both FE pairs and thus the right-hand side of (21) is also the same. At the same time, we get from (7) and the L^2-orthogonality of $\mathbb{Q}_h$ and $\widetilde{\mathbb{Q}}$:

$$\|\tilde{p}\| = \|p - p^h\| = \inf_{q_h \in \mathbb{Q}_h} \|p - q^h\| \approx \begin{cases} h^{k+1}|p|_{H^{k+1}(\Omega)} & \text{for } P_k - P_k, \\ h^k |p|_{H^k(\Omega)} & \text{for } P_k - P_{k-1}. \end{cases}$$

Assume pressure solution p to be sufficiently smooth, such that $c^*|p|_{H^{k+1}(\Omega)} = |p|_{H^k(\Omega)}$ with some finite constant $c^* = O(1)$, which has the physical dimension of the length-scale. In this case, norms of subgrid pressures for equal order $\tilde{p}_{eo}$ and Taylor–Hood $\tilde{p}_{th}$ would scale as

$$c^*\|\tilde{p}_{eo}\| \approx h\|\tilde{p}_{th}\|. \tag{22}$$

This indicates that (21) and so (20) could not be relevant in all situations unless parameters γ_K account on the order of velocity *and* pressure elements or depend on some norms of the unknown continuous solution.

Assume that (19) is appropriate for equal order elements, which is not unreasonable since (19) has been also derived for equal-order elements by other approaches [18,34]. Then, due to (22) and (21), it is natural to introduce for Taylor–Hood (or similar) elements the extra scaling of γ with h^{-1}. On the elementwise level this would lead to $\gamma_K \simeq c^*(\nu h_K^{-1} + \|\mathbf{a}\|_K)$. The latter choice is not optimal, however, for the Stokes case ($\mathbf{a} = 0$), see Section 3.2. Hence, based on the bound (54), we assume

$$\gamma_K \simeq \nu + c^*\|\mathbf{a}\|_K \tag{23}$$

to be a reasonable choice for different order velocity–pressure elements. The above considerations suggest that the best choice of c^* depends on the behavior of the pressure on element K. Since this information is in general not available, we set c^* to be a global constant of order 1. Furthermore, numerical experiments with inf–sup stable $Q_2 - Q_1$ elements from Section 5 clearly show the h-independence of optimal (in the sense of minimizing certain error norms) parameters γ's. Hence the design (23) is more plausible for LBB stable elements compared to (19).

The above discussion shows that, within the variational multiscale framework, the choice of the best parameter γ_K is still an issue. In our opinion, the Assumption 2 might be too strong in some cases since it decouples the resolution of pressure and velocity. Probably, it is advantageous to replace the block-diagonal approximation of $\mathscr{L}$ on K by a block-triangular or another approximation which accounts for both, momentum and continuity residuals, in a subgrid pressure model. This would lead, however, to a bulk of additional terms in the variational FE formulation. We will study such a model elsewhere. In this paper, we attempt to cure the situation by applying different designs of parameters γ_K depending on the relative order of FE pairs.

3. Grad-div stabilization and finite element error analysis

3.1. Preliminaries

The finite element velocity and pressure spaces are based on polynomials of degrees k and s, respectively. Since we avoid using additional pressure stabilization we assume the discrete LBB condition

$$\sup_{\mathbf{u}_h \in \mathbf{V}_h} \frac{(\operatorname{div}\mathbf{u}_h, p_h)}{\|\nabla \mathbf{u}_h\|} \geqslant c_0\|p_h\| \quad \forall p_h \in \mathbb{Q}_h \tag{24}$$

to be valid with a constant c_0 independent of h. Throughout the paper $\|\cdot\|$ denotes the norm in $L^2(\Omega)$ and $H^0 := L^2(\Omega)^d$. The following approximation properties of FE spaces are standard: There exist interpolation operators $I_u : \mathbf{V} \to \mathbf{V}_h$ and $I_p : \mathbb{Q} \to \mathbb{Q}_h$, such that for sufficiently smooth $\mathbf{v}$ and q and any $K \in \mathscr{T}_h$

$$\begin{aligned} &\|\mathbf{v} - I_u\mathbf{v}\|_{H^\ell(K)} \lesssim h_K^{k+1-\ell}|\mathbf{v}|_{H^{k+1}(K)}, \quad \ell = 0, 1, \\ &\|q - I_p q\|_{H^0(K)} \lesssim h_K^{s+1}|p|_{H^{s+1}(K)}. \end{aligned} \tag{25}$$

Moreover, if $\operatorname{div}\mathbf{v} = 0$, then in the first estimate from (25), the interpolant $I_u\mathbf{v}$ can be assumed to belong to the subspace $\mathbf{V}_h^0 := \{\mathbf{v}_h \in \mathbf{V}_h | (\operatorname{div}\mathbf{v}_h, q_h) = 0, \ \forall q_h \in \mathbb{Q}_h\}$ and the norm on the right-hand side is replaced by $|\mathbf{v}|_{H^{k+1}(\widetilde{K})}$, where $\widetilde{K}$ is a suitable neighborhood of K, cf. [21].

For a given triangulation $\mathscr{T}_h$, denote by γ a piecewise constant non-negative function with respect to the partitioning $\mathscr{T}_h$, i.e. $\gamma(\mathbf{x})|_K = \gamma_K \geqslant 0$ for any $K \in \mathscr{T}_h$, where $\{\gamma_K\}$ is a set of constants. Denote

$$\gamma_{\min} = \min_{\mathbf{x}\in\Omega} \gamma(\mathbf{x}), \quad \gamma_{\max} = \max_{\mathbf{x}\in\Omega} \gamma(\mathbf{x}).$$

On $\mathbf{V}$ and $\mathbb{Q}$, we introduce the norms:

$$\|\mathbf{v}\|_V := \left(\nu\|\nabla\mathbf{v}\|^2 + \|\gamma^{\frac{1}{2}}\operatorname{div}\mathbf{v}\|^2\right)^{\frac{1}{2}}, \quad \|q\|_Q := \sup_{\mathbf{v}\in\mathbf{V}} \frac{(\operatorname{div}\mathbf{v}, q)}{\|\mathbf{v}\|_V}. \tag{26}$$

On the product space $\mathbf{V} \times \mathbb{Q}$, we define the product norm

$$|[\mathbf{v}, q]| = \left(\|\mathbf{v}\|_V^2 + \|q\|_Q^2\right)^{\frac{1}{2}},$$

and the bilinear form

$$\begin{aligned} &a_\gamma(\mathbf{u}, p; \mathbf{v}, q) \\ &\quad = \nu(\nabla\mathbf{u}, \nabla\mathbf{v}) + (\gamma\operatorname{div}\mathbf{u}, \operatorname{div}\mathbf{v}) + (\mathbf{a}\cdot\nabla\mathbf{u}, \mathbf{v}) - (p, \operatorname{div}\mathbf{v}) + (q, \operatorname{div}\mathbf{u}). \end{aligned}$$

The discrete problem with grad–div stabilization is given by: Find $\mathbf{u}_h \in \mathbf{V}_h, \ p_h \in \mathbb{Q}_h$ such that

$$a_\gamma(\mathbf{u}_h, p_h; \mathbf{v}_h, q_h) = (\mathbf{f}, \mathbf{v}_h) \quad \forall\ \mathbf{v}_h \in \mathbf{V}_h, \ \ q_h \in \mathbb{Q}_h. \tag{27}$$

Thanks to (24) there is a unique solution to (27). Note that $(\gamma\operatorname{div}\mathbf{u}_h, \operatorname{div}\mathbf{v}_h)$ is the γ-term in (4) or (18).

Besides the product norm $|[\cdot,\cdot]|$ defined above we endow each FE subspace pair $\mathbf{V}_h \times \mathbb{Q}_h$ with the product norm:

$$|[\mathbf{v}_h, q_h]|_h = \left(\|\mathbf{v}_h\|_V^2 + \|q_h\|_{Q_h}^2\right)^{\frac{1}{2}} \quad \text{with } \|q\|_{Q_h} := \sup_{\mathbf{v}_h\in\mathbf{V}_h} \frac{(\operatorname{div}\mathbf{v}_h, p_h)}{\|\mathbf{v}_h\|_V}.$$

The latter relation defines a norm on $\mathbb{Q}_h$ due to the LBB condition (24).

Assume $\gamma > 0$ and consider the constant d_0 defined through the following inf–sup relation:

$$d_0 = \inf_{p_h\in\mathbb{Q}_h} \sup_{\mathbf{u}_h\in\mathbf{V}_h} \frac{(\operatorname{div}\mathbf{u}_h, p_h)}{\|\gamma^{-\frac{1}{2}}p_h\|\|\gamma^{\frac{1}{2}}\operatorname{div}\mathbf{u}_h\|}. \tag{28}$$

For the sake of analysis, we assume that

$$0 < c \leqslant d_0 \tag{29}$$

holds with some mesh -and parameter-independent constant c.

Remark 2. Assumption (29) is quite plausible. Thanks to $\|\operatorname{div}\mathbf{v}\| \leqslant \|\nabla\mathbf{v}\|$ for $\mathbf{v} \in \mathbf{V}$ and (24), we have the obvious bound $0 < c_0(\frac{\gamma_{\min}}{\gamma_{\max}})^{\frac{1}{2}} \leqslant d_0$ and the assumption is trivially fulfilled for $\gamma = \text{const}$. Otherwise d_0 may depend on the *variation* of γ. The following analysis shows that this dependence is very mild: In [13] and [23] the preconditioning for the Stokes problem with variable viscosity was studied. Its performance and analysis relies on an estimate from below for the constant $\widetilde{d}_0$ defined through

$$\widetilde{d}_0 = \inf_{p_h\in\widetilde{\mathbb{Q}}_h} \sup_{\mathbf{u}_h\in\mathbf{V}_h} \frac{(\operatorname{div}\mathbf{u}_h, p_h)}{\|\gamma^{-\frac{1}{2}}p_h\|\|\gamma^{\frac{1}{2}}\mathbf{D}\mathbf{u}_h\|}. \tag{30}$$

where $\mathbf{D}\mathbf{u} = \frac{1}{2}(\nabla\mathbf{u} + \nabla^T\mathbf{u})$ is the rate of deformation tensor (and $\gamma > 0$ has the physical meaning of variable viscosity). Due to $\|\gamma^{\frac{1}{2}}\operatorname{div}\mathbf{u}\| \leqslant \|\gamma^{\frac{1}{2}}\mathbf{D}\mathbf{u}\|$, we get $\widetilde{d}_0 \leqslant d_0$. Numerical experiments with highly variable γ in [23] (for the regularized Bingham models) and [13] (for geophysical models of magma migration and mantle convection) suggest that $\widetilde{d}_0$ is almost insensitive to variations of γ. Furthermore, some lower bounds for the continuous counterpart (30) can be found in [23]. Moreover, the continuous counterpart of (29) trivially gives $d_0 \equiv 1$ with $\mathbb{Q} = \{q \in L^2(\Omega) | \int_\Omega \gamma^{-1}q\,d\mathbf{x} = 0\}$, since in this case $\gamma^{-1}\cdot\mathbb{Q} \subset \Im(\operatorname{div}|_V)$.

In order to avoid the repeated use of generic but unspecified constants, further by $x \lesssim y$ we mean that there is a constant c such that $x \leqslant cy$, and c does not depend of the parameters which x, y may depend on, e.g. ν, $\{\gamma_K\}$, $\mathbf{a}$, and mesh size. Obviously, $x \gtrsim y$ is defined as $y \lesssim x$, and $x \simeq y$ when both $x \lesssim y$ and $y \lesssim x$.

The following Lemma provides some technical results.

Lemma 1. *Assume (24) and (29). Then there holds*

$$\|(\nu+\gamma)^{-\frac{1}{2}}p_h\| \simeq \|p_h\|_{Q_h} \simeq \|p_h\|_Q \quad \forall p_h \in \mathbb{Q}_h. \tag{31}$$

and

$$\|p\|_Q \lesssim \|(\nu+\gamma)^{-\frac{1}{2}}p\| \quad \forall p \in \mathbb{Q}. \tag{32}$$

Proof. Applying the Cauchy inequality and the inequality $\|\operatorname{div}\mathbf{v}\| \leqslant \|\nabla\mathbf{v}\|$ for $\mathbf{v} \in \mathbf{V}$, we get

$$\|p\|_Q = \sup_{\mathbf{v}\in\mathbf{V}} \frac{(\operatorname{div}\mathbf{v}, p)}{\|\mathbf{v}\|_V} \leqslant \sup_{\mathbf{v}\in\mathbf{V}} \frac{\|(\nu+\gamma)^{\frac{1}{2}}\operatorname{div}\mathbf{v}\|\|(\nu+\gamma)^{-\frac{1}{2}}p\|}{\|\mathbf{v}\|_V} \leqslant \|(\nu+\gamma)^{-\frac{1}{2}}p\|.$$

Thus, (32) is proved. The bound $\|p_h\|_{Q_h} \lesssim \|p_h\|_Q$ immediately follows from the definition of the norms and the embedding $\mathbf{V}_h \subset \mathbf{V}$. To prove (31) it remains to show, for arbitrary $p_h \in \mathbb{Q}_h$, the following estimate

$$\|(\nu+\gamma)^{-\frac{1}{2}}p_h\| \lesssim \|p_h\|_{Q_h} = \sup_{\mathbf{v}_h\in\mathbf{V}_h} \frac{(\operatorname{div}\mathbf{v}_h, p_h)}{\sqrt{\nu\|\nabla\mathbf{v}_h\|^2 + \|\gamma^{\frac{1}{2}}\operatorname{div}\mathbf{v}_h\|^2}}. \tag{33}$$

The key relation below follows from the theory of sums and intersections of vector spaces, see the Appendix A:

$$\sup_{\mathbf{v}_h\in\mathbf{V}_h} \frac{(\operatorname{div}\mathbf{v}_h, p_h)}{\sqrt{\nu\|\nabla\mathbf{v}_h\|^2 + \|\gamma^{\frac{1}{2}}\operatorname{div}\mathbf{v}_h\|^2}} = \inf_{q_h\in\mathbb{Q}_h}\left(\sup_{\mathbf{v}_h\in\mathbf{V}_h} \frac{(\operatorname{div}\mathbf{v}_h, p_h - q_h)^2}{\nu\|\nabla\mathbf{v}_h\|^2} + \sup_{\mathbf{v}_h\in\mathbf{V}_h} \frac{(\operatorname{div}\mathbf{v}_h, q_h)^2}{\|\gamma^{\frac{1}{2}}\operatorname{div}\mathbf{v}_h\|^2}\right)^{\frac{1}{2}}. \tag{34}$$

Due to (24) and (29) we get from (34)

$$\sup_{\mathbf{v}_h\in\mathbf{V}_h} \frac{(\operatorname{div}\mathbf{v}_h, p_h)}{\sqrt{\nu\|\nabla\mathbf{v}_h\|^2 + \|\gamma^{\frac{1}{2}}\operatorname{div}\mathbf{v}_h\|^2}} \gtrsim \inf_{q_h\in\mathbb{Q}_h}\left(\nu^{-1}\|p_h - q_h\|^2 + \|\gamma^{-\frac{1}{2}}q_h\|^2\right)^{\frac{1}{2}}. \tag{35}$$

An elementary variation analysis shows that the minimum on the right-hand side of (35) is attained for $q_h = \left(\frac{\gamma}{\nu+\gamma}\right)^{\frac{1}{2}}p_h$. This leads to

$$\inf_{q_h\in\mathbb{Q}_h}\left(\nu^{-1}\|p_h - q_h\|^2 + \|\gamma^{-\frac{1}{2}}q_h\|^2\right)^{\frac{1}{2}} = \|(\nu+\gamma)^{-\frac{1}{2}}p_h\|.$$

This together with (35) proves (33) and so (31). The lemma is proved. □

Remark 3. Consider the operator $S := \operatorname{div}(-\nu\Delta - \nabla\gamma\operatorname{div})^{-1}\nabla$, where $-(\nu\Delta + \nabla\gamma\operatorname{div})^{-1}$ is the solution operator to

$$-\nu\Delta\mathbf{u} - \nabla\gamma\operatorname{div}\mathbf{u} = \mathbf{f} \quad \text{in } \Omega,$$
$$\mathbf{u} = 0 \quad \text{on } \partial\Omega.$$

Since γ is not necessarily continuous, the problem should be understood in the weak sense. One can easily check that S is a self-adjoint positive definite operator on $\mathbb{Q}$ and

$$(Sq, q) = \|q\|_Q^2 \quad \text{for } q \in \mathbb{Q}. \tag{36}$$

Thus the $\|\cdot\|_Q$-norm can be observed as the norm induced by the pressure Schur complement matrix of the linearized problem (5) for $\mathbf{a} = 0$. Similar observation w.r.t. the algebraic Schur complement operator holds for the $\|\cdot\|_{Q_h}$-norm.

We will refer to the following H^2-*regularity condition*: The domain Ω is such that the Stokes problem (i.e. Eq. (5) with $\nu = 1$ and $\mathbf{a} = 0$) is H^2-regular, i.e., there are constants c_u and c_p such that, for any $\mathbf{f} \in L^2(\Omega)^d$, the solution $\{\mathbf{u}, p\}$ is an element of $H^2(\Omega)^d \times H^1(\Omega)$ and satisfies

$$\|\mathbf{u}\|_{H^2(\Omega)} \leqslant c_u\|\mathbf{f}\|, \quad \|\nabla p\| \leqslant c_p\|\mathbf{f}\|. \tag{37}$$

The condition is satisfied for convex domains [15].

3.2. Stokes problem

First we treat the case of the Stokes problem, i.e. $\mathbf{a} = 0$. Although the ∇div-stabilization is usually not applied to the Stokes problem (see, however, [19,41]), we begin our analysis with treating this case, since the problem is symmetric and accurate optimal bounds can be attained. The norms in (26) are based on the "velocity part" of the Stokes problem and its pressure Schur complement operator (cf. Remark 3). In this way, the γ-dependence is taken into account in the norms and the uniform stability and continuity results for $a_\gamma(\cdot;\cdot)$ in (38)–(40) easily follow from an abstract analysis as, for example, in [8]. It holds

$$a_\gamma(\mathbf{u}, p; \mathbf{v}, q) \lesssim |[\mathbf{u}, p]||[\mathbf{v}, q]| \quad \forall\{\mathbf{u}, p\},\ \{\mathbf{v}, q\} \in \mathbf{V}\times\mathbb{Q} \tag{38}$$

$$|[\mathbf{u}, p]| \lesssim \sup_{\mathbf{v},q\in\mathbf{V}\times\mathbb{Q}} \frac{a_\gamma(\mathbf{u}, p; \mathbf{v}, q)}{|[\mathbf{v}, q]|} \quad \forall\{\mathbf{u}, p\} \in \mathbf{V}\times\mathbb{Q} \tag{39}$$

as well as

$$|[\mathbf{u}_h, p_h]|_h \lesssim \sup_{\mathbf{v}_h, q_h \in \mathbf{V}_h \times \mathbb{Q}_h} \frac{a_\gamma(\mathbf{u}_h, p_h; \mathbf{v}_h, q_h)}{|[\mathbf{v}_h, q_h]|_h} \quad \forall \{\mathbf{u}_h, p_h\} \in \mathbf{V}_h \times \mathbb{Q}_h. \tag{40}$$

Remark 4. Using the L^2 norm for the pressure instead of $\|\cdot\|_Q$ and $\|\cdot\|_{Q_h}$ in general leads to parameter dependent stability and continuity constants, see [41].

Further in this section, we prove several FE convergence results for the grad–div stabilized Stokes problem.

Theorem 2. *Assume (24), (29) and* $\mathbf{a} = 0$. *Let* $(\mathbf{u}, p)$ *be a solution to (6) and* $(\mathbf{u}_h, p_h)$ *a solution of (27), then it holds*

$$|[\mathbf{u} - \mathbf{u}_h, p - p_h]| \simeq \inf_{\mathbf{v}_h \in \mathbf{V}_h} \inf_{q_h \in \mathbb{Q}_h} |[\mathbf{u} - \mathbf{v}_h, p - q_h]|. \tag{41}$$

Assume further the H^2*-regularity condition and* $\max_{K \in \mathcal{T}_h} h_K \leqslant h$, *then*

$$\|\mathbf{u} - \mathbf{u}_h\| \lesssim \left(\frac{c_u^2 (\nu + \gamma_{\max})}{\nu^2} + \frac{c_p^2}{\nu + \gamma_{\min}} \right)^{\frac{1}{2}} h |[\mathbf{u} - \mathbf{u}_h, p - p_h]|. \tag{42}$$

Proof. Let $\mathbf{u}_I$ be the best approximation to $\mathbf{u}$ in $\mathbf{V}_h$ with respect to the $\|\cdot\|_V$ norm and p_I be the best approximation to p in $\mathbb{Q}_h$ with respect to the $\|\cdot\|_Q$ norm. The norm equivalence (31), stability (40), continuity (38) estimates, and the orthogonality property of the FE error function give:

$$\begin{aligned}
|[\mathbf{u}_I - \mathbf{u}_h, p_I - p_h]| &\lesssim |[\mathbf{u}_I - \mathbf{u}_h, p_I - p_h]|_h \\
&\lesssim \sup_{\mathbf{v}_h, q_h \in \mathbf{V}_h \times \mathbb{Q}_h} \frac{a_\gamma(\mathbf{u}_I - \mathbf{u}_h, p_I - p_h; \mathbf{v}_h, q_h)}{|[\mathbf{v}_h, q_h]|_h} \\
&\lesssim \sup_{\mathbf{v}_h, q_h \in \mathbf{V}_h \times \mathbb{Q}_h} \frac{a_\gamma(\mathbf{u}_I - \mathbf{u}_h, p_I - p_h; \mathbf{v}_h, q_h)}{|[\mathbf{v}_h, q_h]|} \\
&= \sup_{\mathbf{v}_h, q_h \in \mathbf{V}_h \times \mathbb{Q}_h} \frac{a_\gamma(\mathbf{u}_I - \mathbf{u}, p_I - p; \mathbf{v}_h, q_h)}{|[\mathbf{v}_h, q_h]|} \\
&\lesssim |[\mathbf{u}_I - \mathbf{u}, p_I - p]|.
\end{aligned}$$

With the help of this estimate and the triangle inequality we get

$$|[\mathbf{u} - \mathbf{u}_h, p - p_h]| \lesssim |[\mathbf{u}_I - \mathbf{u}, p_I - p]| = \inf_{\mathbf{v}_h \in \mathbf{V}_h} \inf_{p_h \in \mathbb{Q}_h} |[\mathbf{u} - \mathbf{v}_h, p - q_h]|.$$

Since $\{\mathbf{u}_h, p_h\} \in \mathbf{V}_h \times \mathbb{Q}_h$ the inverse inequality

$$\inf_{\mathbf{v}_h \in \mathbf{V}_h} \inf_{p_h \in \mathbb{Q}_h} |[\mathbf{u} - \mathbf{v}_h, p - q_h]| \lesssim |[\mathbf{u} - \mathbf{u}_h, p - p_h]|$$

is evident. The equivalence (41) is proved.

With the help of a standard duality argument we prove (42). Denote $\mathbf{e}_h = \mathbf{u} - \mathbf{u}_h,\ r_h = p - p_h$. Consider $\mathbf{w} \in H^2(\Omega)^d,\ q \in H^1(\Omega) \cap \mathbb{Q}$ solving the Stokes problem

$$-\nu\Delta\mathbf{w} - \nabla q = \mathbf{e}_h, \quad \operatorname{div}\mathbf{w} = 0 \quad \text{in } \Omega,$$
$$\mathbf{w} = 0 \quad \text{on } \partial\Omega.$$

Thanks to the H^2-regularity assumption, the following *a priori* estimate holds

$$\nu\|\mathbf{w}\|_{H^2} \leqslant c_u \|\mathbf{e}_h\|, \quad \|\nabla q\| \leqslant c_p \|\mathbf{e}_h\|. \tag{43}$$

Using the weak form of the problem and the orthogonality property for $\mathbf{e}_h, r_h$, we get

$$\|\mathbf{e}_h\|^2 = a_\gamma(\mathbf{w} - \mathbf{w}_h, q - q_h; \mathbf{e}_h, r_h)$$

with arbitrary $\mathbf{w}_h \in \mathbf{V}_h,\ q_h \in \mathbb{Q}_h$. Thanks to (38), (32), interpolation properties (25), and *a priori* estimate (43), we obtain

$$\begin{aligned}
\|\mathbf{e}_h\|^2 &\lesssim |[\mathbf{w} - \mathbf{w}_h, q - q_h]| |[\mathbf{e}_h, r_h]| \\
&\lesssim (\|\mathbf{w} - \mathbf{w}_h\|_V^2 + \|(\nu + \gamma)^{-\frac{1}{2}}(q - q_h)\|^2)^{\frac{1}{2}} |[\mathbf{e}_h, r_h]| \\
&\lesssim ((\nu + \gamma_{\max})\|\nabla(\mathbf{w} - \mathbf{w}_h)\|^2 + (\nu + \gamma_{\min})^{-1}\|q - q_h\|^2)^{\frac{1}{2}} |[\mathbf{e}_h, r_h]| \\
&\lesssim h((\nu + \gamma_{\max})\|\mathbf{w}\|_{H^2}^2 + (\nu + \gamma_{\min})^{-1}\|\nabla q\|^2)^{\frac{1}{2}} |[\mathbf{e}_h, r_h]| \\
&\lesssim \left(c_u^2 \frac{\nu + \gamma_{\max}}{\nu^2} + \frac{c_p^2}{\nu + \gamma_{\min}} \right)^{\frac{1}{2}} h \|\mathbf{e}_h\| |[\mathbf{e}_h, r_h]|.
\end{aligned}$$

Thus (42) is proved. □

Theorem 2, interpolation properties (25), and estimate (32) immediately yield the following corollary.

Corollary 3. *Let* $(\mathbf{u}, p)$ *be a smooth solution to (6) and* $(\mathbf{u}_h, p_h)$ *a solution of (27), then the following error estimate holds*

$$|[\mathbf{u} - \mathbf{u}_h, p - p_h]|^2 \lesssim \sum_{K \in \mathcal{T}_h} h_K^{2k} \left((\nu + \gamma_K)|\mathbf{u}|_{H^{k+1}(K)}^2 + \frac{1}{\nu + \gamma_K} |p|_{H^k(K)}^2 \right) \tag{44}$$

Finding the minimum of the right-hand side from (44) with respect to γ_K gives the optimal value

$$\gamma_K \simeq \max\left\{ \frac{|p|_{H^k(K)}}{|\mathbf{u}|_{H^{k+1}(K)}} - \nu, 0 \right\}. \tag{45}$$

Remark 5. The assumption (29) can be avoided. In this case, one can show (see, e.g. [20]):

$$\|\mathbf{u} - \mathbf{u}_h\|_V^2 + \frac{1}{\nu + \gamma_{\max}} \|p - p_h\|^2 \lesssim \inf_{\mathbf{v}_h \in \mathbf{V}_h} \inf_{q_h \in \mathbb{Q}_h} |[\mathbf{u} - \mathbf{v}_h, p - q_h]|. \tag{46}$$

The norm on the left-hand side of (46) is somewhat weaker than in (41). More important, however, is that (41) gives the *equivalence* result, while (46) is only the upper bound. Thus the bound in the $|[\cdot,\cdot]|$ norm is tight. This suggests that the choice of γ's from (45) is likely to minimize the left-hand side in (41) as well.

Since the norms of solution on the right-hand side of (45) are not accessible, different assumptions and/or simplifications can be made to obtain computable expressions for γ_K. Below we review few different approaches to handle this problem.

- *Regularity based approach* is typical for analysis in the framework of least-squares and Petrov-Galerkin methods [20,34,44,47]. Based on the regularity theory for the Navier-Stokes equations, one assumes that for many flows of interest $\|\mathbf{u}\|_{H^{k+1}(\widetilde{T})} \approx \|p\|_{H^k(\widetilde{T})}$, which yields for small enough ν the choice
$$\gamma_K \simeq 1. \tag{47}$$
This choice, however, is rather questionable for the Stokes problem alone, since the resulting method does not pass the simple scaling criteria: for $\mathbf{u} \to \lambda\mathbf{u}$ the parameters should scale like $\nu \to \lambda^{-1}\nu$ and $\gamma \to \lambda^{-1}\gamma$. We will revisit this approach for the Oseen problem below.
- In the **f**-*based approach* one supposes that some *a priori* estimates provide useful information about the unknown solution. Thus the regularity estimate for the Stokes problem gives: $\nu\|\mathbf{u}\|_{H^{k+1}(\Omega)} \leqslant \tilde{c}_u \|\mathbf{f}\|_{H^{k-1}(\Omega)}$ and $\|p\|_{H^k(\Omega)} \leqslant \tilde{c}_p \|\mathbf{f}\|_{H^{k-1}(\Omega)}$. Therefore, the error estimate (44) yields
$$|[\mathbf{u} - \mathbf{u}_h, p - p_h]|^2 \lesssim h^{2k} \left(\frac{\tilde{c}_u^2 (\nu + \gamma_{\max})}{\nu^2} + \frac{\tilde{c}_p^2}{\nu + \gamma_{\min}} \right) \|\mathbf{f}\|_{H^{k-1}(\Omega)}^2$$
An optimal parameter is given now by the choice
$$\gamma_K \simeq \max\{(\tilde{c}_p \tilde{c}_u^{-1} - 1)\nu, 0\}. \tag{48}$$
Note that, for the Stokes problem, (48) is similar to the choice of $\gamma \simeq \nu$ based on the bubble functions enrichment [19] and the analysis of the SUPG method for equal-order velocity–pressure elements [18].
- One may also think of an L^2-norm approach based on the estimate (42) for the L_2-norm of velocity. Thus, instead of minimizing the error estimate in the ν-dependent norm as in (44), one may minimize the right-hand side of (42) assuming that the $|[\cdot,\cdot]|$-norm of the error is almost γ-independent (the assumption is somewhat vague, of course). This also leads to (48).

The situation for the "simple" case of the Stokes problem is now clear: there is the optimal choice of γ's in (45), which can be simplified in different ways depending on some *a priori* knowledge of the solution behavior. Further we extend the above analysis to the Oseen problem ($\mathbf{a}$ is not necessarily zero). We shall see that similar conclusions hold in this more general case.

3.3. Oseen problem: $\mathbf{a}\neq 0$

Most of the analysis for the Stokes problem from the previous section can be extended to the Oseen equations. However, the optimality (tightness) of the error representation as in (41) will be lost since the problem is not symmetric anymore.

In addition to the norms used before we will need the following norm on $\mathbf{V}$:

$$\|\mathbf{v}\|_a := \left(\|\mathbf{v}\|_V^2 + \nu^{-1}\|\mathbf{a}\otimes\mathbf{v}\|^2\right)^{\frac{1}{2}}.$$

The product space norm in this section is altered by the $\mathbf{a}$-dependent scaling of the pressure norm:

$$|[\mathbf{v},q]|_a := \left(\|\mathbf{v}\|_V^2 + c_p(\nu+\gamma_{\max}+\nu^{-1}\|\mathbf{a}\|_\infty^2)^{-1}\|q\|^2\right)^{\frac{1}{2}}$$

with an appropriate mesh- and parameter-independent constant $c_p > 0$.

Remark 6. The error for the Oseen problem will be estimated in the $|[\cdot,\cdot]|_a$ norm defined above. If we also assume the alternative inf–sup condition for $\mathbb{Q}_h \subset H^1(\Omega)$:

$$\sup_{\mathbf{u}_h\in\mathbf{V}_h}\frac{(\operatorname{div}\mathbf{u}_h, p_h)}{\|\mathbf{u}_h\|} \geqslant \tilde{c}_0\|\nabla p_h\| \quad \forall p_h\in\mathbb{Q}_h, \tag{49}$$

then the error analysis can be done with the stronger pressure norm:

$$\|q\|_a^2 := \sup_{\mathbf{v}\in\mathbf{V}_h}\frac{(\operatorname{div}\mathbf{v},q)^2}{\|\mathbf{v}\|_V^2+\nu^{-1}\|\mathbf{a}\|_\infty^2\|\mathbf{v}\|^2}$$

instead of $(\nu+\gamma_{\max}+\nu^{-1}\|\mathbf{a}\|_\infty^2)^{-1}\|q\|^2$. Condition (49) is satisfied by Taylor–Hood or Mini element [42,36]. However, we shall not elaborate details, since this improvement is tangential to the main topic of the paper.

The following result generalizes Theorem 2 for the Stokes problem.

Theorem 4. *Let $(\mathbf{u},p)$ be a solution to (6) and $(\mathbf{u}_h,p_h)$ a solution of (27). Then it holds*

$$|[\mathbf{u}-\mathbf{u}_h,p-p_h]|_a \lesssim \left(\inf_{\mathbf{v}_h\in\mathbf{V}_h}\|\mathbf{u}-\mathbf{v}_h\|_a^2 + \inf_{q_h\in\mathbb{Q}_h}\|(\nu+\gamma)^{-\frac{1}{2}}(p-q_h)\|^2\right)^{\frac{1}{2}}. \tag{50}$$

Proof. The result is a special case of [37] where additionally a reduced variant of the streamline-diffusion stabilization is considered. Following [37], we obtain in the first step the stability estimate

$$a_\gamma(\mathbf{v}_h,q_h;\mathbf{v}_h,q_h) \geqslant \frac{1}{2}|[\mathbf{v}_h,q_h]|_a^2 \quad \forall(\mathbf{v}_h,q_h)\in\mathbf{V}_h\times\mathbb{Q}_h. \tag{51}$$

Let $\mathbf{u}_J = I_u\mathbf{u}$ be the interpolant to $\mathbf{u}$ in $\mathbf{V}_h$ with the divergence-preserving interpolation operator I_u of Girault–Scott [21]. Moreover, let p_I be the best approximation to p in $\mathbb{Q}_h$. Using the property $(q_h, \operatorname{div}(\mathbf{u}-\mathbf{u}_J)) = 0$, we obtain in a second step the estimate

$$\begin{aligned} a_\gamma(\mathbf{u}-\mathbf{u}_J,p-p_I;\mathbf{v}_h,q_h) &\leqslant \|\mathbf{u}-\mathbf{u}_J\|_{\mathbf{V}}|[\mathbf{v}_h,q_h]|_a + (p-p_I,\operatorname{div}\mathbf{v}_h) - (\mathbf{a}\otimes(\mathbf{u}-\mathbf{u}_J),\nabla\mathbf{v}_h) \\ &\lesssim (\|\mathbf{u}-\mathbf{u}_J\|_a^2 + \|(\nu+\gamma)^{-\frac{1}{2}}(p-p_I)\|^2)^{\frac{1}{2}}|[\mathbf{v}_h,q_h]|_a. \end{aligned} \tag{52}$$

Then we set $(\mathbf{v}_h,q_h) = (\mathbf{u}_h-\mathbf{u}_J, p_h-p_I)$ and derive from (51), (52), together with the Galerkin orthogonality $a_\gamma(\mathbf{u}-\mathbf{u}_h,p-p_h;\mathbf{v}_h,q_h)=0$, the estimate:

$$|[\mathbf{u}_h-\mathbf{u}_J,p_h-p_I]|_a \lesssim (\|\mathbf{u}-\mathbf{u}_J\|_a^2 + \|(\nu+\gamma)^{-\frac{1}{2}}(p-p_I)\|^2)^{\frac{1}{2}}.$$

The triangle inequality concludes the proof of (50). □

Corollary 5. *Let $(\mathbf{u},p)$ be a smooth solution to (6) and $(\mathbf{u}_h,p_h)$ a solution of (27). Then it holds*

$$|[\mathbf{u}-\mathbf{u}_h,p-p_h]|_a^2 \lesssim \sum_{K\in\mathcal{T}_h} h_K^{2k}\left(\left(\nu+\gamma_K+\frac{h_K^2|\mathbf{a}|_K^2}{\nu}\right)|\mathbf{u}|_{H^{k+1}(\widetilde{K})}^2 + \frac{1}{\nu+\gamma_K}|p|_{H^k(K)}^2\right) \tag{53}$$

with $|\mathbf{a}|_K := \|\mathbf{a}\|_{L^\infty(K)}^2$.

Proof. The interpolation property (25) for the pressure and the corresponding estimates for the divergence-constraint preserving interpolator I_u, see (25), immediately yield the bound (53). □

Finding the minimum of the right-hand side from (53) with respect to γ_K gives the optimal value in (45) up to the extension of the velocity semi-norm to a neighborhood $\widetilde{K}$ of K. Attempting to deduce computable expression for γ_K, one may follow the same arguments as for the Stokes case:

- Assuming $\|\mathbf{u}\|_{H^{k+1}(\widetilde{K})} \approx \|p\|_{H^k(K)}$ together with the scaling of equation in a way that $\|\mathbf{a}\| = 1$ (for some norm of $\mathbf{a}$) yields the choice $\gamma_K \simeq 1$ again. This design of γ's can be found in [20,29,37,44]. The drawback of this parameter design is that the local behavior of flow is not taken into account.
- Compared to the Stokes problem it is not easy to obtain sharp estimates for the higher derivatives of $\mathbf{u}$ and p due to the presence of the convection term $\mathbf{a}\cdot\nabla\mathbf{u}$. In the case when the contribution of body forces $\mathbf{f}$ in the momentum can be neglected, the approximate equality $-\nu\Delta\mathbf{u}+\mathbf{a}\cdot\nabla\mathbf{u} \approx \nabla p$ yields

  $$|p|_{H^k(K)} \lesssim \nu|\mathbf{u}|_{H^{k+1}(\widetilde{K})} + \sum_{m=0}^{k-1}\|\mathbf{a}\|_{W^{m,\infty}(\widetilde{K})}|\mathbf{u}|_{H^{k-m}(\widetilde{K})}.$$

  Now assume that the bounds $|\mathbf{u}|_{H^{k-m}(\widetilde{K})} \leqslant c_m|\mathbf{u}|_{H^{k+1}(\widetilde{K})}$ hold with some finite constants c_m, which have dimension of $[\text{length-scale}]^{m+1}$. This provides the upper bound for optimal parameters

  $$\gamma_K \lesssim \left(\nu + \sum_{m=0}^{k-1}c_m\|\mathbf{a}\|_{W^{m,\infty}(\widetilde{K})}\right). \tag{54}$$

  Note that the design deduced in the multiscale framework in (23):

  $$\gamma_K \simeq \nu + c^*\|\mathbf{a}\|_K \tag{55}$$

  perfectly fits the condition (54) for $k = 1$.
- Finally, note that the Dirichlet inflow boundary conditions for (5) lead to Dirichlet outflow boundary conditions and thus poor regularity for the adjoint problem. Then, we are not able to deduce reasonable formulas for γ_K based on a L^2-norm error estimate for $\mathbf{a}\neq 0$.

Remark 7. The above analysis suggests that for shear/channel flows where the inertia terms $\mathbf{a}\cdot\nabla\mathbf{u}$ vanish the estimate (54) is not sharp in its $\mathbf{a}$-dependent part and thus the design (55) is not perfect. This explains the well-known numerical observation (see, e.g. [33]) that for laminar channel flows the choice $\gamma \simeq \nu$ is optimal, which is in contrast to flows with an intense inertia phenomenon, see examples in Section 5. For flow exhibiting mixed dynamics or in the lack of additional information about the continuous problem solution $\{\mathbf{u}, p\}$, the design of the stabilization parameter γ is a controversial issue. Thus, there is no surprise that different recommendations can be found in the literature. To amend this situation one may try a 'dynamic' choice of parameter γ directly based on (45) setting, for example,

$$\gamma_K \simeq \max\left\{\frac{|p^*|_{H^k(\widetilde{K})}}{|\mathbf{u}^*|_{H^{k+1}(\widetilde{K})}} - \nu, 0\right\}, \tag{56}$$

where $\widetilde{K}$ is a macro-element such that $K \subset \widetilde{K}$, and $\mathbf{u}^*, p^*$ are approximations to $\mathbf{u}_h$, p_h from the previous Picard iteration or time step, that the semi-norms in (56) makes sense. Some other approximations to (45) can be considered as well.

Remark 8. The norm of the velocity error on the left-hand side of (50) depends on ν and γ. For $\gamma = 0$ the estimate allows the $O(\nu^{-1})$ scaling of the velocity error with respect to the best possible pressure approximation. Note that in the Stokes case such estimate is optimal, cf. (41). For $\gamma = O(1)$ only $O\left(\nu^{-\frac{1}{2}}\right)$ scaling of the velocity error is allowed by (50). Moreover, in this case one gets additional control of mass conservation for the discrete solution. In particular, for $\gamma = O(1)$ estimate (50) implies

$$\|\mathrm{div}\,\mathbf{u}_h\| \lesssim \left(\inf_{\mathbf{v}_h \in \mathbf{V}_h} \|\mathbf{u} - \mathbf{v}_h\|_a^2 + \inf_{q_h \in \mathbb{Q}_h} \|p - q_h\|^2\right)^{\frac{1}{2}}.$$

3.4. Equal order elements

The error estimates (44) and (53) and hence the basic formula (45) were deduced for the case of different order LBB stable velocity and pressure elements. Here we extend the analysis to pressure-stabilized discretizations of the Oseen problem which allow equal-order pairs. The error analysis basically follows the lines of Section 3.3, so we outline the necessary modifications. To avoid additional, but non-important for our purpose complications, we assume that the convection is not numerically dominant, i.e. $|\mathbf{a}|_K h_K \leqslant \frac{1}{2}\nu$ for all elements K and $\mathbb{Q}_h \subset H^1(\Omega)$. The bilinear form of the pressure stabilized FE method is augmented with an additional term as:

$$a_\gamma^{st}(\mathbf{u}_h, p_h; \mathbf{v}_h, q_h) := a_\gamma(\mathbf{u}_h, p_h; \mathbf{v}_h, q_h) + \sum_{K \in \mathcal{T}_h} \tau_K \int_K (-\nu\Delta\mathbf{u}_h + \mathbf{a}\cdot\nabla\mathbf{u}_h + \nabla p_h)\cdot\nabla q_h\,\mathrm{d}\mathbf{x}$$

and the discrete problem now reads: Find $\mathbf{u}_h \in \mathbf{V}_h, p_h \in \mathbb{Q}_h$ such that

$$a_\gamma^{st}(\mathbf{u}_h, p_h; \mathbf{v}_h, q_h) = (\mathbf{f}, \mathbf{v}_h) + \sum_{K \in \mathcal{T}_h} \tau_K \int_K \mathbf{f}\cdot\nabla q_h\,\mathrm{d}\mathbf{x} \quad \forall \mathbf{v}_h \in \mathbf{V}_h,\ q_h \in \mathbb{Q}_h. \tag{57}$$

Following [14], the stabilization parameter is designed through $\tau_K \simeq h_K^2(\nu + |\mathbf{a}|_K h_K)^{-1}$. The product norm is altered as

$$|[\mathbf{v}, q]|_{st}^2 := \left(\|\mathbf{v}\|_V^2 + c_p(\nu + \gamma_{\max} + \nu^{-1}\|\mathbf{a}\|_\infty^2)^{-1}\|q\|^2 + \sum_{K \in \mathcal{T}_h} \tau_K \|\nabla q\|_K^2\right)^{\frac{1}{2}}.$$

Instead of the LBB condition (24) we need the following weak inf–sup condition (e.g. [5]):

$$\sup_{\mathbf{u}_h \in \mathbf{V}_h} \frac{(\mathrm{div}\,\mathbf{u}_h, p_h)}{\|\nabla\mathbf{u}_h\|} \geqslant c_0\|p_h\| - c_1\left(\sum_{K \in \mathcal{T}_h} h_K^2 \|\nabla p_h\|_K^2\right)^{\frac{1}{2}} \quad \forall p_h \in \mathbb{Q}_h \tag{58}$$

with positive constants c_0, c_1 independent of h. Following the same arguments as in [37], we obtain the stability estimate

$$a_\gamma^{st}(\mathbf{v}_h, q_h; \mathbf{v}_h, q_h) \geqslant c|[\mathbf{v}_h, q_h]|_{st}^2 \quad \forall (\mathbf{v}_h, q_h) \in \mathbf{V}_h \times \mathbb{Q}_h$$

with some positive parameter independent constant c. Further, repeating arguments from the proof of Theorem 4, we get the error estimate

$$|[\mathbf{u} - \mathbf{u}_h, p - p_h]|_{st} \lesssim \left(\inf_{\mathbf{v}_h \in \mathbf{V}_h} \|\mathbf{u} - \mathbf{v}_h\|_a^2 + \inf_{q_h \in \mathbb{Q}_h}\left\{\|(\nu+\gamma)^{-\frac{1}{2}}(p - q_h)\|^2 + \sum_{K \in \mathcal{T}_h} \tau_K \|\nabla(p - q_h)\|_K^2\right\}\right)^{\frac{1}{2}},$$

where $(\mathbf{u}, p)$ and $(\mathbf{u}_h, p_h)$ are solutions to (6) and (57), respectively. Interpolation properties of FE spaces now yield

$$|[\mathbf{u} - \mathbf{u}_h, p - p_h]|_{st}^2 \lesssim \sum_{K \in \mathcal{T}_h} h_K^{2k}\left(\left(\nu + \gamma_K + \frac{h_K^2|\mathbf{a}|_K^2}{\nu}\right)|\mathbf{u}|_{H^{k+1}(\widetilde{K})}^2 + \frac{h_K^2}{\nu + \gamma_K}|p|_{H^{k+1}(K)}^2 + \tau_K|p|_{H^{k+1}(K)}^2\right).$$

Thus, if *equal-order elements* are used, then the error analysis leads to the different optimal parameter:

$$\gamma_K \simeq \max\left\{h_K\frac{|p|_{H^{k+1}(K)}}{|\mathbf{u}|_{H^{k+1}(\widetilde{K})}} - \nu, 0\right\}. \tag{59}$$

For *smooth solutions*, this would scale the parameter from (45) with h_K. Note that this conclusion is similar to the one obtained by different arguments within the variational multiscale framework of Section 2.

The next section studies dissipation properties of the grad–div stabilization.

4. Numerical dissipation vs. mass balance for grad–div terms

In this section, we show that in general the grad–div stabilization introduces some numerical dissipation into the method. In particular, this suggests an explanation why such grad–div enhancement alone was shown to be useful for stable calculations of turbulent solutions, see [29]. Introducing too large numerical dissipation is also related to over-stabilization effects when γ is taken too large, see numerical examples in the next section. Let $\mathbf{u}_h(t)$ be the FE solution to (4). Assuming the skew-symmetric approximation of the convection term, the discrete energy balance for $\mathbf{u}_h(t)$ is given by

$$\|\mathbf{u}_h(t)\|^2 + \nu\int_0^t \|\nabla\mathbf{u}_h(s)\|^2\,\mathrm{d}s + \int_0^t \|\gamma^{\frac{1}{2}}\mathrm{div}\,\mathbf{u}_h(s)\|^2\,\mathrm{d}s = \|\mathbf{u}_h(0)\|^2 + (\mathbf{f}, \mathbf{u}_h(t)) \quad \text{for } t \in (0, T]. \tag{60}$$

The second term in (60) corresponds to the viscous dissipation of the energy, while the third term in (60) (non-negative for all t and thus potentially dissipative) has no matching in the energy balance for the continuous solution. Thus the rate of numerical dissipation introduced by the grad–div stabilization at time t can be measured as

$$\mathrm{diss}(t) = \frac{\|\gamma^{\frac{1}{2}}\mathrm{div}\,\mathbf{u}_h(t)\|^2}{\|\nabla\mathbf{u}_h(t)\|^2}. \tag{61}$$

Let $\mathbf{V}_h^0 := \{\mathbf{v}_h \in \mathbf{V}_h | (\mathrm{div}\,\mathbf{v}_h, q_h) = 0,\ \forall q_h \in \mathbb{Q}_h\}$ be the set of discrete divergence free velocity functions. Since the solution $\mathbf{u}_h(t)$ belongs to $\mathbf{V}_h^0$, the quantities

$$\mu_h = \inf_{\mathbf{v}_h \in \mathbf{V}_h^0} \frac{\|\gamma^{\frac{1}{2}}\mathrm{div}\,\mathbf{v}_h\|}{\|\nabla\mathbf{v}_h\|} \quad \text{and} \quad M_h = \sup_{\mathbf{v}_h \in \mathbf{V}_h^0} \frac{\|\gamma^{\frac{1}{2}}\mathrm{div}\,\mathbf{v}_h\|}{\|\nabla\mathbf{v}_h\|} \tag{62}$$

give us bounds for the numerical diffusion from (61):

$$\mu_h^2 \leqslant \mathrm{diss}(t) \leqslant M_h^2.$$

Denote by G the FE matrix representation of the grad–div term.

When numerically evaluating μ_h^2 with element order $p \geqslant 2$, there are true divergence-free functions in $\mathbf{V}_h^0$, thus μ_h would be zero (see Figs. 1 and 2). We can still calculate the minimal diffusion on the complementary orthogonal subspace $\mathbf{V}_h^0 \setminus \ker(G)$ to gain some insight. For this we look at the quantity

$$\tilde{\mu}_h = \inf_{\mathbf{v}_h \in \mathbf{V}_h^0 \setminus ker(G)} \frac{\|\gamma^{\frac{1}{2}} \mathrm{div}\, \mathbf{v}_h\|}{\|\nabla \mathbf{v}_h\|}$$

instead of the lower bound μ_h.

For the following calculation we assume $\gamma = 1$ and denote the FE matrices for the diffusion and divergence terms with A and B, respectively. Further, let P be the L^2-orthogonal projection from $\mathbf{V}_h$ onto $\mathbf{V}_h^0$. The matrix counterpart of this projection will be also denoted by P, thus P is the orthogonal projector from $\mathbb{R}^n$ onto $V^0 := ker(B)$. Note that $P\,G$ is a symmetric operator on V^0 and $P\,A$ is a symmetric positive definite operator on V^0.

Now the bounds M_h^2 and μ_h^2 can be expressed via generalized Rayleigh quotients:

$$M_h^2 = \sup_{\mathbf{v}_h \in \mathbf{V}_h^0} \frac{\|\gamma^{\frac{1}{2}} \mathrm{div}\, \mathbf{v}_h\|^2}{\|\nabla \mathbf{v}_h\|^2} = \max_{u \in V^0} \frac{\langle Gu, u\rangle}{\langle Au, u\rangle} = \max_{u \in V^0} \frac{\langle PGu, u\rangle}{\langle PAu, u\rangle} =: \lambda_{\max},$$

$$\mu_h^2 = \inf_{\mathbf{v}_h \in \mathbf{V}_h^0} \frac{\|\gamma^{\frac{1}{2}} \mathrm{div}\, \mathbf{v}_h\|^2}{\|\nabla \mathbf{v}_h\|^2} = \min_{u \in V^0} \frac{\langle Gu, u\rangle}{\langle Au, u\rangle} = \min_{u \in V^0} \frac{\langle PGu, u\rangle}{\langle PAu, u\rangle} =: \lambda_{\min},$$

and can be determined by the minimal and maximal eigenvalues $\lambda_{\min}$ and $\lambda_{\max}$ of

$$\lambda PAu = PGu, \quad u \in V^0. \tag{63}$$

By the definition of P, $Pv = 0$ is equivalent to $v = B^T q$ with some $q \in \mathbb{R}^m$. This makes (63) equivalent to

$$\begin{pmatrix} G & 0 \\ 0 & 0 \end{pmatrix} \begin{pmatrix} v \\ p \end{pmatrix} = \lambda \begin{pmatrix} A & B^T \\ B & 0 \end{pmatrix} \begin{pmatrix} v \\ p \end{pmatrix}, \quad v \neq 0, \tag{64}$$

which can be solved with a generalized eigenvalue solver. In Fig. 2, one can see the spectra for different element orders and mesh refinements. In Table 1, we present our results of lower and upper bounds for the numerical dissipation for different element orders and refinements; '*'-sign means that computing the whole spectra for this case was beyond available computer resources.

We can draw a few observations and conclusions from these results. Table 1 shows that for Q_1 velocity approximation at least $O(\gamma h^2)$ numerical dissipation is introduced. Note that Q_1 velocities can be used with both LBB unstable equal order and LBB stable iso $Q_2 - Q_1$ and iso $Q_2 - Q_0$ elements. For higher order elements, numerical dissipation acts only on a subspace of $\mathbf{V}_h^0$. The relative dimension of this subspace decreases and the relative dimension of the strongly divergence-free velocity subspace increases for higher order elements. Fig. 2 and Table 1 show that for certain modes the $O(\gamma)$ numerical dissipation is introduced; the properties of these modes and the relation of such anisotropic non-uniform dissipation to the turbulence modeling character of the grad–div stabilization deserves further studies. At the same time, the existence of eigenmodes of (63) with $\lambda = O(1)$ warns us against possible over-diffusion (over-stabilization) for larger γ's.

Note that the FE method imposes only global mass balance through the identity $(\mathrm{div}\, \mathbf{u}_h, q_h) = 0$ for all $q_h \in \mathbb{Q}_h$. The resulting FE solution is not necessarily div-free since $\mathrm{div}\,(\mathbf{V}_h) \notin \mathbb{Q}_h$, and even element-wise mass balance can be violated if $\mathbb{Q}_h$ does not contain piecewise constant functions (as, for example, happens with Taylor–Hood elements). Another role of the grad–div stabilization is to enforce mass balance in a stronger way. This can be seen in two ways; more investigation in this direction can be found in [32]. First of all, as already discussed in Remark 8, the stabilization leads to a better scaled estimate of $\|\mathrm{div}\, \mathbf{u}_h\|$. Also, assuming $\gamma = $ const and $\mathbf{u}_h \in \mathbf{V}_h^0$, it holds:

$$\|\gamma^{\frac{1}{2}} \mathrm{div}\, \mathbf{u}_h\|^2 = \gamma(\mathrm{div}\, \mathbf{u}_h, \mathrm{div}\, \mathbf{u}_h - q_h) \quad \forall q_h \in \mathbb{Q}_h$$

Therefore

$$\|\gamma^{\frac{1}{2}} \mathrm{div}\, \mathbf{u}_h\| = \gamma^{\frac{1}{2}} \inf_{q_h \in \mathbb{Q}_h} \|\mathrm{div}\, \mathbf{u}_h - q_h\| \quad \forall \mathbf{u}_h \in \mathbf{V}_h^0 \tag{65}$$

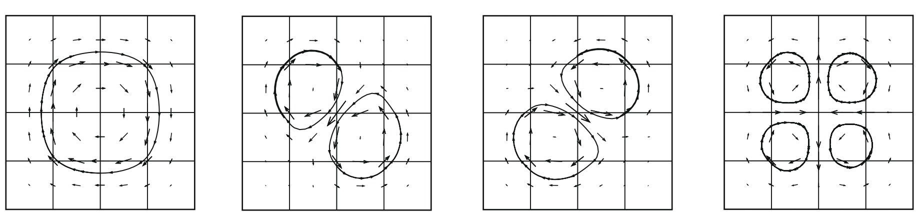

Fig. 1. Four basis functions of the (strongly) divergence-free subspace for Q_2 and $h = 1/4$.

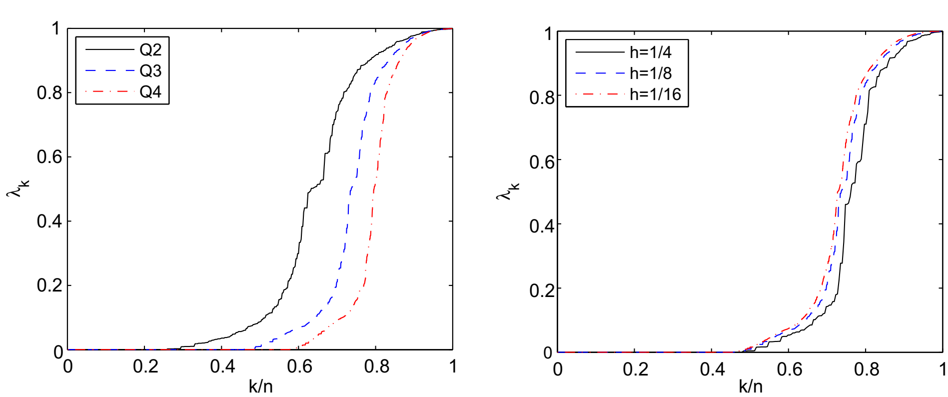

Fig. 2. Eigenvalue spectra for different element orders and $h = 1/8$ (left) and for Q3 with different refinements (right). X-axis is rescaled to $[0, 1]$.

Table 1
Dimension of truly div-free functions subspace of $\mathbf{V}_h^0(\mathbf{G} = \ker G)$ and bounds for numerical dissipation on its orthogonal complement subspace in $\mathbf{V}_h^0$.

h	1/4	1/8	1/16	1/32
	Q_1			
$\dim(\mathbf{G})/\dim(\mathbf{V}_h)$	0/ 18	0/ 98	0/ 450	0/ 1922
μ_h^2	4.8812e−2	1.1864e−2	2.9564e−3	7.3869e−4
	Q_2			
$\dim(\mathbf{G})/\dim(\mathbf{V}_h^0/\mathbf{G})$	4/ 94	36/ 414	196/ 1726	900/ 7038
$\tilde{\mu}_h^2$	8.9596e−3	2.4653e−3	6.3427e−4	1.6002e−4
M_h^2	9.9302e−1	9.9961e−1	9.9998e−1	1.0000e−0
	Q_3			
$\dim(\mathbf{G})/\dim(\mathbf{V}_h^0/\mathbf{G})$	36/ 206	196/ 862	900/ 3518	*/ *
$\tilde{\mu}_h^2$	4.3242e−3	1.0953e−3	2.7497e−4	6.9336e−5
M_h^2	9.9876e−1	9.9992e−1	9.9999e−1	1.0000e−0
	Q_4			
$\dim(\mathbf{G})/\dim(\mathbf{V}_h^0/\mathbf{G})$	100 / 350	484 / 1438	2116 / 5822	* / *
$\tilde{\mu}_h^2$	2.4296e−3	6.1053e−4	1.5289e−4	3.8241e−5
M_h^2	9.9955e−1	9.9997e−1	1.0000e−0	1.0000e−0

and the stabilization can be also observed as a way to penalize the discrepancy between $\operatorname{div}(\mathbf{V}_h)$ and $\mathbb{Q}_h$.

Summarizing the above discussion, we may consider the search of optimal parameters γ as *a trade-off between mass and energy balance* in the FE system.

5. Numerical experiments

Let us start with two examples for the Oseen problem (5) where the grad–div parameter is designed according to (56) or according to the simplified settings $\gamma_K = \gamma_0(\nu + \|\mathbf{a}\|_K)$ and $\gamma_K \equiv \gamma_0$. We note that, although the latter choice does not account for the local behavior of flow, it has the following attractive property: the additional stabilization matrix should be assembled only once, while (23) requires the matrix to be updated every time step or every non-linear iteration. In either case γ_0 is an additional parameter, which has to be specified. The calculation in all examples were performed with Q_2/Q_1-approximations for velocity/pressure with the grad–div stabilized Galerkin scheme using the library `deal.II` [1].

Example 1. We solve the Oseen problem on $\Omega = (0,1)^2$ for viscosity $\nu = 10^{-6}$ with the flow field $\mathbf{a}(x) = (\sin(2\pi x_1)\cos(2\pi x_2), -\cos(2\pi x_1)\sin(2\pi x_2))^T$, source term $\mathbf{f}(x) := 8\pi^2\nu b(x)$, but with inhomogeneous Dirichlet data $\mathbf{u}(x) = \mathbf{a}(x)$ on $\partial\Omega$. The exact solution $\mathbf{u}(x) := \mathbf{a}(x)$ and $p(x) := \frac{1}{4}(\cos(4\pi x_1) + \cos(4\pi x_2))$ is smooth and ν-independent. For this example there holds $(\mathbf{u}\cdot\nabla)\mathbf{u} = \pi(\sin(4\pi x_1), -\sin(4\pi x_2))^T$. Moreover, one observes a strong variation of the mesh Reynolds number $Re_K := \frac{\|\mathbf{u}\|_{\infty,K} h_K}{\nu}$ over the domain between 0 and $\frac{h_K}{\nu}$.

We present in Fig. 3 the plots of the H^1- and L^2-errors for the solution with the "dynamic" variant of the grad–div stabilization according to the optimal choice (56), i.e., with $\gamma_K = \tilde{\gamma}_0 \frac{|p|_{H^2(K)}}{|\mathbf{u}|_{H^3(K)}}$. The seminorms in (56) were approximated using the 1-st order quadrature formulas and the explicitly computed higher order derivatives for given pressure and velocity solution. We observe a distinguished and h-independent minimum of the errors for parameter $\tilde{\gamma}_0 \approx 1$ which leads (as compared to the unstabilized case) to improved values of the norms by a factor of nearly 10^{-2} on the finest grid. In the paper we discussed several simplified designs for γ_K. In numerical experiments we try the constant choice and (23).

Thus, we present in Fig. 4 the plots of the H^1- and L^2-errors for the solution with the simple grad–div stabilization, i.e., with $\gamma_K = \gamma_0$. We observe again a distinguished and h-independent minimum of the errors for parameter $\gamma_0 \approx 10^{-1}$ which leads to very similar results as for the "dynamic" choice. Note that $\max_K \frac{|p|_{H^2(K)}}{|\mathbf{u}|_{H^3(K)}} \approx 10^{-1}$ which explains that $\gamma_0 \approx 0.1\tilde{\gamma}_0$.

Further, we show in Fig. 5 the corresponding plots of the H^1- and L^2-errors for the solution with different values of viscosity ν and fixed $h \approx \frac{1}{64}$. We observe that the pronounced and h-independent minimum of the errors is more and more pronounced with decreasing ν. At the same time, no degradation of the error occurs in the diffusion-dominated case.

The results for this example suggest that a globally constant value of the grad–div parameter γ_0 is reasonable and, of course, much cheaper than the "dynamic" design.

Example 2. As a second example, we consider a problem with a boundary layer proposed in [4]. We solve the Oseen problem on $\Omega = (0,1)^2$ with $\mathbf{a} = \mathbf{u}$ and solution

$$u_1(x) = \left(1 - \cos\left(\frac{2\pi(e^{R_1 x_1} - 1)}{e^{R_1} - 1}\right)\right) \sin\left(\frac{2\pi(e^{R_2 x_2} - 1)}{e^{R_2} - 1}\right) \frac{R_2}{2\pi} \frac{e^{R_2 x_2}}{(e^{R_2} - 1)},$$

$$u_2(x) = -\sin\left(\frac{2\pi(e^{R_1 x_1} - 1)}{e^{R_1} - 1}\right)\left(1 - \cos\left(\frac{2\pi(e^{R_2 x_2} - 1)}{e^{R_2} - 1}\right)\right) \frac{R_1}{2\pi} \frac{e^{R_1 x_1}}{(e^{R_1} - 1)},$$

$$p(x) = R_1 R_2 \sin\left(\frac{2\pi(e^{R_1 x_1} - 1)}{e^{R_1} - 1}\right) \sin\left(\frac{2\pi(e^{R_2 x_2} - 1)}{e^{R_2} - 1}\right) \frac{e^{R_2 x_1} e^{R_2 x_2}}{(e^{R_1} - 1)(e^{R_2} - 1)}.$$

The velocity field resembles a counter-clockwise vortex with the center at

$$(x_{01}, x_{02}) = \left(\frac{1}{R_1} \log\left(\frac{e^{R_1} + 1}{2}\right), \frac{1}{R_2} \log\left(\frac{e^{R_2} + 1}{2}\right)\right).$$

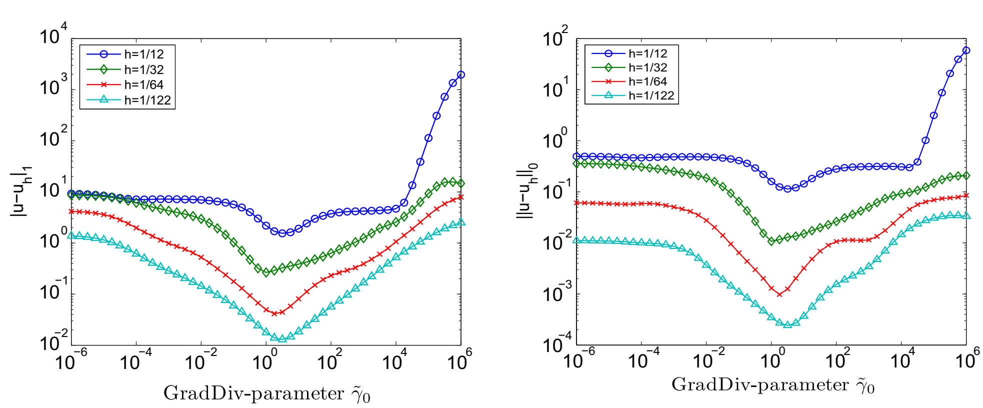

Fig. 3. Plots of H^1- and L^2-errors vs. scaling parameter $\tilde{\gamma}_0$ of "dynamic" grad–div stabilization for Example 1 with $\nu = 10^{-6}$, $\sigma = 0$ and different values of h.

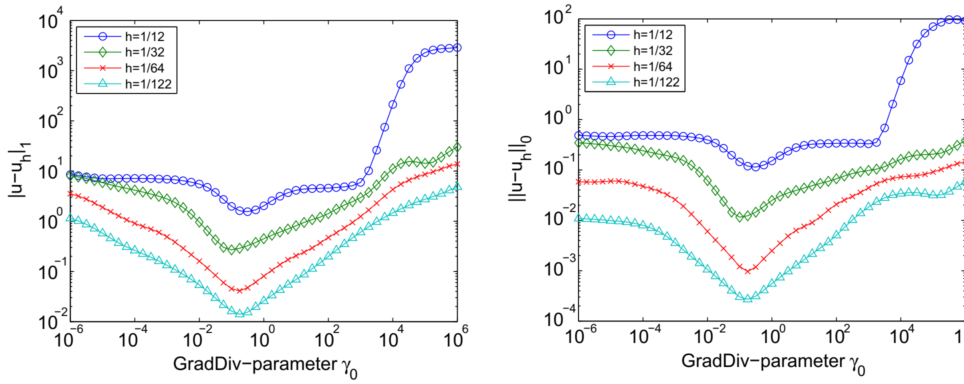

Fig. 4. Plots of H^1- and L^2-errors vs. scaling parameter γ_0 of grad–div stabilization for Example 1 with $\nu = 10^{-6}$, $\sigma = 0$ and different values of h.

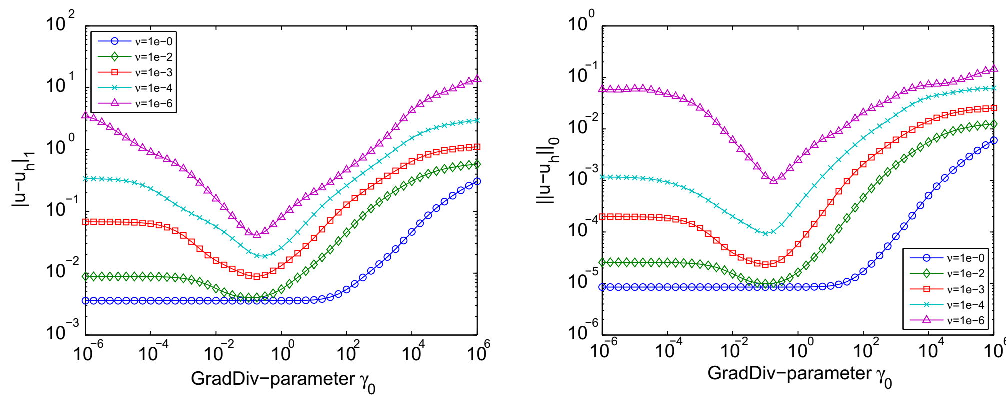

Fig. 5. Plots of H^1- and L^2-errors vs. scaling parameter γ_0 of grad–div stabilization for Example 1 with different values of ν and $\sigma = 0$, $h \approx \frac{1}{64}$.

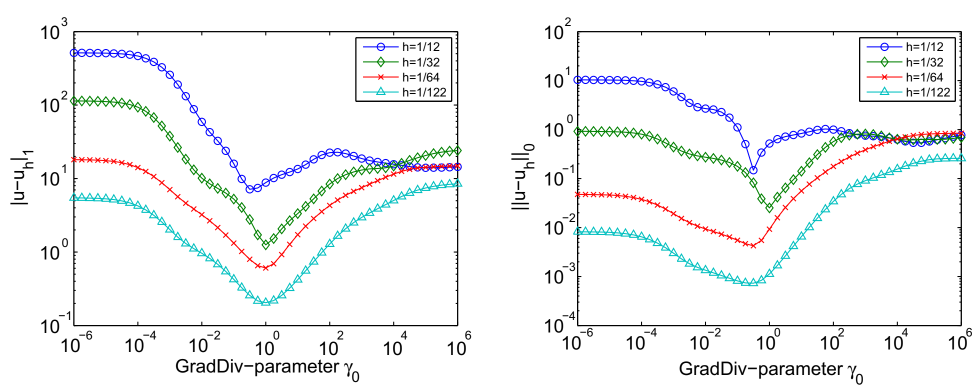

Fig. 6. Errors in H^1-seminorm and L^2-norm vs. scaling parameter γ_0 of grad–div stabilization for Example 2 with $\nu = 10^{-4}$ and different values of h.

The parameters are chosen as $R_2 = 0.1$ leading to $x_{02} = 0.5125$ and R_1 such that $x_{01} = 1 - \nu^{\frac{1}{4}}$, i.e. the center moves with decreasing ν to the right boundary. This leads to a ν-dependent solution with $\|\nabla \mathbf{u}\|_0 \sim \nu^{-0.35}$ and $\|p\|_0 \sim \nu^{-0.12}$.

In Fig. 6, we present results for $\nu = 10^{-4}$ and $\gamma_K = \gamma_0(\nu + \|\mathbf{a}\|_K)$. The value of the viscosity allows a resolution of the boundary layer on the finest meshes. The errors in the H^1-seminorm and L^2-norm are again plotted against the scaling parameter γ_0. The tests reflect again robustness of the discrete solution with respect to γ_0 and a pronounced, *h-independent minimum*. In comparison to the unstabilized case $\gamma_0 = 0$, we observe for an optimal value of γ_0 a reduction of the errors on the finer meshes by a factor of nearly 10^{-2}. This reduction is clearly pronounced as in Example 1. We note that the simplified choice $\gamma_K = \gamma_0$ was found for this problem to produce very similar results.

Remark 9. Results in Figs. 4 and 6 show that the optimal value of γ_0 is problem dependent, which is a typical situation with any stabilization parameter. We have no *a priori* rule how to pick up the optimal value of γ_0 for a given problem. Although in the log-scale of Figs. 4 and 6 the minima with respect to the variation of γ_0 looks rather sharp, the results suggest that any *a priori* choice of $\gamma_0 \in [0.1, 1]$ is not overstabilizing and would lead to a significant improvement in accuracy compared to the unstabilized problem.

Example 3. As a last example, we consider the time-dependent Navier-Stokes flow of generalized Beltrami type, see [16]. This flow is defined in $\Omega = (-1, 1)^3$. The exact solution is

$$u(t,x) = -a\begin{pmatrix} e^{ax_1}\sin(ax_2+bx_3) + e^{ax_3}\cos(ax_1+bx_2) \\ e^{ax_2}\sin(ax_3+bx_1) + e^{ax_1}\cos(ax_2+bx_3) \\ e^{ax_3}\sin(ax_1+bx_2) + e^{ax_2}\cos(ax_3+bx_1) \end{pmatrix} e^{-b^2\nu t}$$

and

$$\begin{aligned} p(t,x) = -\frac{1}{2}a^2[&e^{2ax_1} + e^{2ax_2} + e^{2ax_3} \\ &+ 2\sin(ax_1+bx_2)\cos(ax_3+bx_1)e^{a(x_2+x_3)} \\ &+ 2\sin(ax_2+bx_3)\cos(ax_1+bx_2)e^{a(x_3+x_1)} \\ &+ 2\sin(ax_3+bx_1)\cos(ax_2+bx_3)e^{a(x_1+x_2)}]e^{-2b^2\nu t} \end{aligned}$$

with parameters $a = \pi/4$ and $b = \pi/2$. This flow is a series of counter-rotating vortices intersecting one another at oblique angles.

The numerical solution is obtained on a series of equidistant meshes with $h = 2^{-k}, k \in \{2, 3, 4, 5\}$. The time discretization is performed by means of a stiff-stable diagonally implicit Runge-Kutta method of order 2 with time step $\Delta t = \frac{1}{64}$. This is sufficient to guarantee that the discretization error in time does not dominate the spatial error.

We present in Fig. 7 (left) the plots of the error in $L^2(\Omega)$ (as function of t) for $Re = 10^6$ and different values of h for the Galerkin scheme, i.e. without grad–div stabilization, (left) and for fixed h and different values of the grad–div parameter (right). The improvement even with the simple (time-independent) grad–div stabilization $\gamma_K = \gamma_0$ is obvious. Moreover, as we observe in the left part, the error with grad–div stabilization for $h = \frac{1}{8}$ is better than the error without stabilization for $h = \frac{1}{16}$. This is a problem reduction by a factor 8.

We present in Fig. 8 (left) the plots of the error in $L^2(\Omega)$ (as function of t) for fixed h and different Reynolds numbers. The case without grad–div stabilization is shown on the left whereas the grad–div stabilized case is presented on the right. Again, the stabilizing influence of grad–div terms is obvious in case of high Reynolds numbers.

6. Summary, outlook

In this paper, we considered the grad–div stabilization as a subgrid pressure model in the framework of variational multiscale methods and critically discussed the choice of corresponding parameters.

For linearized problems of Stokes and Oseen type, we derived refined error estimates of the grad–div stabilized method in the case of inf–sup stable and equal-order interpolations of velocity/pressure. It turns out that the design of the set of stabilization parameters for inf–sup stable elements differs from the case of equal-order elements. Unfortunately, the optimized parameters depend on the (unknown) solution. Therefore, we discussed some variants of a simplified parameter design. Both the analysis and numerical experiments show that for inf–sup stable elements the optimal choice of the stabilization parameters is h-independent.

Moreover, we discussed the influence of the grad–div stabilization terms on energy and mass balance of the discrete flow problem. Finally, some numerical experiments for the Oseen and the Navier-Stokes problem support the theoretical considerations. In

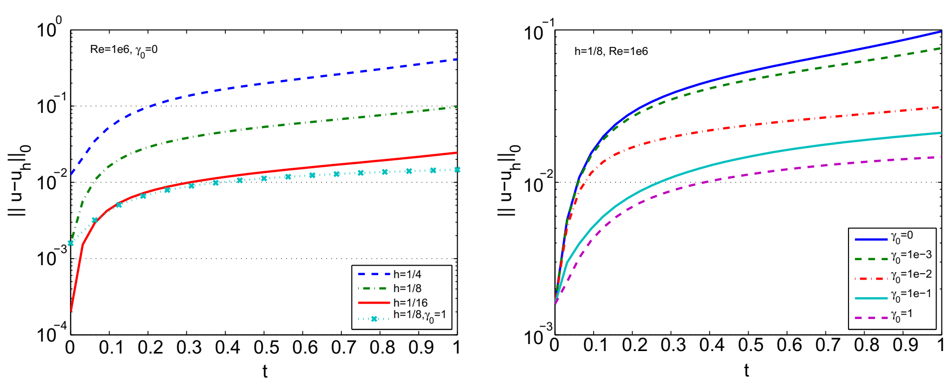

Fig. 7. Error in L^2-norm vs. $t \in [0, 1]$ without stabilization for different values of h (left) and with grad–div stabilization for fixed h for $\nu = 10^{-6}$ for Example 3.

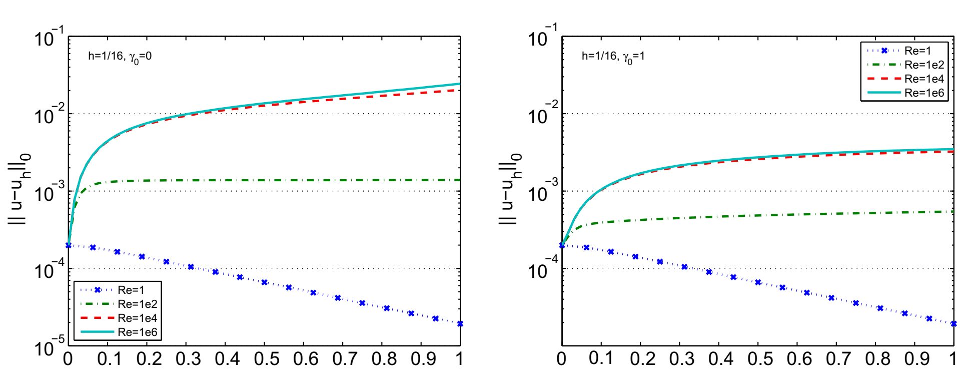

Fig. 8. Error in L^2-norm vs. $t \in [0, 1]$ for different values of $Re = \frac{1}{\nu}$ without stabilization (left) and with grad–div stabilization (right) for Example 3.

future research, it seems to be important to study the role of grad–div stabilization as a subgrid pressure model for turbulent flows.

Appendix A

We use the concept of sums and intersections of vector spaces (cf. [3]). Let X, Y be compatible normed spaces, i.e., both X and Y are subspaces of some larger topological vector space Z. Then we can form their sum $X+Y$ and intersection $X\cap Y$. The sum $X+Y$ consists of all $z\in Z$ such that $z=x+y$ with $x\in X,\ y\in Y$. The spaces $X\cap Y$ and $X+Y$ are normed vector spaces with norms

$$\|x\|_{X\cap Y}=\left(\|x\|_X^2+\|x\|_Y^2\right)^{\frac{1}{2}}\quad (x\in X\cap Y)$$
$$\|z\|_{X+Y}=\inf_{z=x+y}\left(\|x\|_X^2+\|y\|_Y^2\right)^{\frac{1}{2}}\quad (x\in X,\ y\in Y).$$

If X and Y are complete then both $X\cap Y$ and $X+Y$ are complete. If X and Y are Hilbert spaces such that $X\cap Y$ is dense in both X and Y, then $(X\cap Y)'=X'+Y'$ holds and

$$\|g\|_{(X\cap Y)'}=\|g\|_{X'+Y'}\quad \text{for all } g\in(X\cap Y)'. \tag{66}$$

Here X' denotes the dual space to X. Proofs of these assertions can be found in [3] or [42].

In the proof of Lemma 1 we apply the result in (66) setting $X=\mathbf{V}_h$ with the norm $\nu^{\frac{1}{2}}\|\nabla\cdot\|$ and $Y=\mathbf{V}_h$ with the norm $(\|\gamma^{\frac{1}{2}}\mathrm{div}\cdot\|^2+\varepsilon\|\cdot\|^2)^{\frac{1}{2}}$ with an arbitrary $\varepsilon>0$. Further, g is the functional on $\mathbf{V}_h$ defined as $\langle g,\mathbf{v}_h\rangle:=(p_h,\mathrm{div}\,\mathbf{v}_h)$ for a given $p_h\in\mathbb{Q}_h$ and any $\mathbf{v}_h\in\mathbf{V}_h$. This leads to

$$\sup_{\mathbf{v}_h\in\mathbf{V}_h}\frac{(\mathrm{div}\,\mathbf{v}_h,p_h)}{\sqrt{\nu\|\nabla\mathbf{v}_h\|^2+\|\gamma^{\frac{1}{2}}\mathrm{div}\,\mathbf{v}_h\|^2+\varepsilon\|\mathbf{v}_h\|^2}}$$
$$=\inf_{q_h\in\mathbb{Q}_h}\left(\sup_{\mathbf{v}_h\in\mathbf{V}_h}\frac{(\mathrm{div}\,\mathbf{v}_h,p_h-q_h)^2}{\nu\|\nabla\mathbf{v}_h\|^2}+\sup_{\mathbf{v}_h\in\mathbf{V}_h}\frac{(\mathrm{div}\,\mathbf{v}_h,q_h)^2}{\|\gamma^{\frac{1}{2}}\mathrm{div}\,\mathbf{v}_h\|^2+\varepsilon\|\mathbf{v}_h\|^2}\right)^{\frac{1}{2}}.$$

Letting $\varepsilon\to 0$ yields the desired relation (34).

References

[1] W. Bangerth, R. Hartmann, G. Kanschat, Deal. II. A general-purpose object-oriented finite element library, ACM Trans. Math. Softw. 33 (4) (2007).
[2] Y. Bazilevs, V.M. Calo, J.A. Cottrell, T.J.R. Hughes, A. Reali, G. Scovazzi, Variational multiscale residual-based turbulence modeling for large eddy simulation of incompressible flows, Comput. Methods Appl. Mech. Engrg. 197 (2007) 173–201.
[3] J. Bergh, J. Löfström, Interpolation Spaces, Springer, Berlin, 1976.
[4] S. Berrone, Adaptive discretization of the Navier–Stokes equations by stabilized finite element methods, Comput. Methods Appl. Mech. Engrg. 190 (2001) 4435–4455.
[5] P.B. Bochev, C.R. Dohrmann, M.D. Gunzburger, Stabilization of low-order mixed finite elements for the Stokes equations, SIAM J. Numer. Anal. 44 (2006) 82–101.
[6] M. Braack, E. Burman, Local projection stabilization for the Oseen problem and its interpretation as a variational multiscale method, SIAM J. Numer. Anal. 43 (2006) 2544–2566.
[7] M. Braack, E. Burman, V. John, G. Lube, Stabilized finite element methods for the generalized Oseen problem, Comput. Methods Appl. Mech. Eng. 196 (2007) 853–866.
[8] F. Brezzi, M. Fortin, Mixed and Hybrid Finite Element Methods, Springer-Verlag, New-York, 1991.
[9] F. Brezzi, L.P. Franca, T.J.R. Hughes, A. Russo, $b=\int g$, Comp. Methods Appl. Mech. Engrg. 145 (1997) 329–339.
[10] F. Brezzi, A. Russo, Choosing bubbles for advection–diffusion problems, Math. Models Methods Appl. Sci. 4 (1994) 571–587.
[11] A. Brooks, T.J.R. Hughes, Streamline upwind/Petrov–Galerkin formulation for convection dominated flows with particular emphasis on the incompressible Navier–Stokes equations, Comput. Methods Appl. Mech. Engrg. 32 (1982) 199–259.
[12] E. Burman, P. Hansbo, Edge stabilization for Galerkin approximations of convection–diffusion–reaction problems, Comput. Methods Appl. Mech. Engrg. 193 (2004) 1437–1453.
[13] C. Burstedde, O. Ghattas, G. Stadler, T. Tu, L.C. Wilcox, Parallel scalable adjoint-based adaptive solution of variable-viscosity Stokes flow problems, Comput. Methods Appl. Mech. Engrg. 198 (2009) 1691–1700.
[14] R. Codina, Stabilized finite element approximation of transient incompressible flows using orthogonal subscales, Comput. Methods Appl. Mech. Engrg. 191 (2002) 4295–4321.
[15] M. Dauge, Stationary stokes Navier–Stokes systems on two- or three-dimensional domains with dorners. Part I. Linearized Equations, SIAM J. Math. Anal. 20 (1989) 74–97.
[16] C. Eithier, D. Steinman, Exact fully 3d Navier-Stokes solutions for benchmarking, Int. J. Numer. Methods Fluids 19 (1994) 369–375.
[17] C. Foias, D.D. Holm, E.S. Titi, The Navier–Stokes-alpha model of fluid turbulence, Phys. D: Nonlinear Phenom. 152 (2001) 505–519.
[18] L.P. Franca, S.L. Frey, Stabilized finite element methods. II. The incompressible Navier–Stokes equations, Comput. Methods Appl. Mech. Engrg. 99 (1992) 209–233.
[19] L.P. Franca, S.P. Oliveira, Pressure bubbles stabilization features in the Stokes problem, Comput. Methods Appl. Mech. Engrg. 192 (2003) 1929–1937.
[20] T. Gelhard, G. Lube, M.A. Olshanskii, J.-H. Starcke, Stabilized finite element schemes with LBB-stable elements for incompressible flows, J. Comput. Appl. Math. 177 (2005) 243–267.
[21] V. Girault, L.R. Scott, A quasi-local interpolation operator preserving the discrete divergence, Calcolo 40 (2003) 1–19.
[22] V. Gravemeier, W.A. Wall, E. Ramm, Large eddy simulation of turbulent incompressible flows by a three-level finite element method, Int. J. Numer. Methods Fluids 48 (2005) 1067–1099.
[23] P.P. Grinevich, M.A. Olshanskii, An iterative method for the Stokes type problem with variable viscosity, SIAM J. Sci. Comp., in press.
[24] P. Hansbo, A. Szepessy, A velocity–pressure streamline diffusion method for the incompressible Navier–Stokes equations, Comput. Methods Appl. Mech. Engrg. 84 (1990) 175–192.
[25] T.J.R. Hughes, L.P. Franca, M. Balestra, A new finite element formulation for computational fluid dynamics.V: circumventing the Babuska–Brezzi condition: a stable Petrov–Galerkin formulation of the Stokes problem accommodating equal-order interpolations, Comput. Methods Appl. Mech. Engrg. 59 (1986) 85–99.
[26] T.J.R. Hughes, L.P. Franca, G.M. Hulbert, A new finite element formulation for computational fluid dynamics: VIII. The Galerkin/least:-squares method for advective–diffusive equations, Comput. Methods Appl. Mech. Engrg. 73 (1989) 173–189.
[27] T.J.R. Hughes, Multiscale phenomena: Green's functions, the Dirichlet-to-Neumann formulation, subgrid scale models, bubbles and the origins of stabilized methods, Comput. Methods Appl. Mech. Engrg. 127 (1995) 387–401.
[28] T.J.R. Hughes, G.R. Feijoo, L. Mazzei, J.-B. Quincy, The variational multiscale method – a paradigm for computational mechanics, Comput. Methods Appl. Mech. Engrg. 166 (1998) 3–24.
[29] V. John, A. Kindl, Numerical studies of finite element variational multiscale methods for turbulent flow simulations, Comput. Methods Appl. Mech. Engrg. (2009), doi:10.1016/j.cma.2009.01.010.
[30] W. Layton, C.C. Manica, M. Neda, M. Olshanskii, L.G. Rebholz, On the accuracy of the rotation form in simulations of the Navier–Stokes equations, J. Comput. Phys. 228 (2009) 3433–3447.
[31] W. Layton, C.C. Manica, M. Neda, L.G. Rebholz, Numerical analysis and computational comparisons of the NS-alpha and NS-omega regularizations, Comput. Methods Appl. Mech. Engrg. (2009), doi:10.1016/j.cma.2009.01.011.
[32] A. Linke, Collision in a cross-shaped domain. A steady 2d Navier–Stokes example demonstrating the importance of mass conservation in CFD, Comput. Methods Appl. Mech. Engrg. (2009), doi:10.1016/j.cma.2009.06.016.
[33] J. Löwe, A locally adapting parameter design for the divergence stabilization of FEM discretizations of the Navier–Stokes equations, in: A. Hegarty et al. (Eds.), BAIL 2008 – Boundary and Interior Layers, Lecture Notes in Computational Science and Engineering, vol. 69, Springer, Berlin, Heidelberg, 2009.
[34] G. Lube, Stabilized Galerkin finite element methods for convection dominated and incompressible flow problems, Numer. Anal. Math. Modell. (29) (1994) 85–104.
[35] A. Masud, R.A. Khurram, A multiscale finite element method for the incompressible Navier–Stokes equations, Comput. Methods Appl. Mech. Engrg. 195 (2006) 1750–1777.
[36] K.-A. Mardal, X.-C. Tai, R. Winther, A robust finite element method for Darcy–Stokes flow, SIAM J. Numer. Anal. (40) (2002) 1605–1631.
[37] G. Matthies, G. Lube, L. Röhe, Some remarks on residual-based stabilisation of inf–sup stable discretisations of the generalised Oseen problem, preprint 2009.
[38] G. Matthies, L. Tobiska, Local projection type stabilization applied to inf–sup stable discretizations of the Oseen problem, Preprint 47/2007, Dept. Math., Otto-von-Guericke-Universitat Magdeburg, 2007.
[39] A.A. Oberai, P.M. Pinsky, A multiscale finite element method for the Helmholz equation, Comput. Methods Appl. Mech. Engrg. 154 (1998) 281–297.
[40] M.A. Olshanskii, A low order Galerkin finite element method for the Navier–Stokes equations of steady incompressible flow: a stabilization issue and iterative methods, Comput. Methods Appl. Mech. Engrg. 191 (2002) 5515–5536.
[41] M.A. Olshanskii, A. Reusken, Grad–Div stabilization for the Stokes equations, Math. Comp. 73 (2004) 1699–1718.
[42] M.A. Olshanskii, J. Peters, A. Reusken, Uniform preconditioners for a parameter dependent saddle point problem with application to generalized Stokes interface equations, Numer. Math. 105 (2006) 159–191.
[43] J. Principe, R. Codina, F. Henke, The dissipative structure of variational multiscale methods for incompressible flows, Comput. Methods Appl. Mech. Engrg. (2009), doi:10.1016/j.cma.2008.09.007.

[44] H.-G. Roos, M. Stynes, L. Tobiska, Robust Numerical Methods for Singulary Perturbed Differential Equations: Convection Diffusion and Flow Problems, Springer Ser. in Comp. Math, 24, Springer, Berlin, Heidelberg, 2008.
[45] D. Silvester, A. Wathen, Fast iterative solution of stabilised stokes systems, Part II: using general block preconditioners, SIAM J. Numer. Anal. 31 (1994) 1352–1367.
[46] P. Sváček, Application of finite element method in aeroelasticity, J. Comput. Appl. Math. 215 (2008) 586–594.
[47] L. Tobiska, R. Verfürth, Analysis of a streamline diffusion finite element method for the Stokes and Navier–Stokes equations, SIAM J. Numer. Anal. 33 (1996) 107–127.